LAPPEENRANTA UNIVERSITY OF TECHNOLOGY
Department of Electrical Engineering

High Performance Electrical Drive System for a Biomechanical Test and Rehabilitation Equipment

A thesis submitted for approval for the degree of
Master of Science in Engineering

Supervisor: Professor Juha Pyrhönen, D.Sc.

Lappeenranta October 31st, 2000

Sami Halabeya

LEIRIKATU 2 D 8
53600 LAPPEENRANTA
FINLAND

ABSTRACT

Author:	Sami Halabeya
Title:	High Performance Electrical Drive System for a Biomechanical Test and Rehabilitation Equipment.
Department:	Department of Electrical Engineering.
Year:	2000
Place:	Lappeenranta, Finland.

Master's Thesis, Lappeenranta University of Technology
71 pages, 25 figures, 21 tables and 5 appendices.

Keywords: induction motor drive, position control, dynamic performance, rehabilitation, exercise machine, motor types

In this thesis, a high performance direct torque controlled induction motor drive was designed and built to replace a passive non-motorized resistive brake mechanism in a biomechanical test and training system used mainly in rehabilitation. Different high performance motors and drives available in the market were studied and compared before selecting the appropriate technology.

A study of two high performance control schemes of induction machine, namely vector control and direct torque control was also given. The components, assembly, and performance test results of the prototype drive in addition to a strict safety plan compose a major part of this thesis.

TIIVISTELMÄ

Tekijä:	Sami Halabeya
Nimi:	Lihasvoiman testaukseen ja kuntoutukseen soveltuvan tehokkaan sähkökäytön kehittäminen.
Työn teettäjä:	Sähkötekniikan osasto.
Vuosi:	2000
Paikka:	Lappeenranta, Suomi.

Diplomityö. Lappeenrannan teknillinen korkeakoulu
71 sivua, 25 kuvaa, 21 taulukkoa ja 5 liitettä.

Hakusanat: oikosulkumoottori, paikoitusohjaus, kuntoutus, lihasvoiman testaus, moottorityypit

Suunniteltiin ja rakennettiin suoraa vääntömomenttisäätöä soveltava taajuudenmuuttajakäyttö oikosulkumoottorin ohjaukseen korvaamaan passiivinen jarrukäyttö. Laite on kuntoutuslaite, jolla tehdään lihasvoiman mittauksia ja voimaharjoituksia. Selvitettiin kaupallisten moottoreiden ja taajuudenmuuttajien suoritusominaisuuksia ja tämän perusteella valittiin käyttöön sopivat laitteet. Työssä esitetään kaksi oikosulkumoottorin ohjaustapaa: vektorisäätö ja suora vääntömomenttisäätö. Merkittävin osa tästä työstä käsittelee - tarkan turvallisuussuunnitelman lisäksi - kuntoutuslaitteen prototyypin komponentteja, kokoamista ja suoritustestien tuloksia.

NOMENCLATURE

B	Flux density
B_{D}	Knee flux density
B_{g}	Air-gap flux density
E	Supply voltage
E_{a}	Back emf of dc machine
f	frequency
I_{a}	Armature current of dc machine
I_{c}	Compensating current of dc machine
I_{f}	Field current
I_{n}	Nominal current
$\hat{I}_{\mathrm{s}}$	Amplitude of the stator current
i_{sd}	Flux producing current component in rotor reference frame
i_{sq}	Torque producing current component in rotor reference frame
$i_{\mathrm{a}}, i_{\mathrm{b}}, i_{\mathrm{c}}$	Instantaneous values of the stator currents in stator phases
$\boldsymbol{i}_{\mathrm{s}}$	Stator current space vector
J	Moment of inertia
L_{a}	Armature inductance
L_{f}	Field inductance
L_{m}	Magnetizing inductance
L_{r}	Rotor inductance
L_{s}	Stator inductance
$L_{\mathrm{sd}}, L_{\mathrm{sq}}$	Direct and quadrature axis inductances of RSM
l_{g}	PMSM air-gap length
l_{m}	PMSM magnetic thickness
m	Mass
n	Gear ratio
n_{m}	Rotor speed
n_{n}	Nominal speed
n_{s}	Synchronous speed
n_{r}	Slip speed
P_{n}	Nominal power
P_{hd}	Heavy duty power
P_{o}	Output power
p	Number of pole pairs
R_{a}	Armature resistance
s	Per unit slip
T_{a}	Acceleration torque
T_{c}	Constant speed torque
T_{d}	Deceleration torque
T_{e}	Electrical output torque
T_{eff}	Effective torque

T_{inertia}	Torque required to accelerate the motor inertia
T_{Lmax}	Maximum load torque
T_{L}	Load torque
T_{m}	The torque developed by the motor
T_{max}	Maximum motor torque
T_{MLmax}	Maximum load torque referred to motor side
T_{n}	Nominal torque
T_{s}	The torque required to drive the load referred to the motor side
t_{a}	Acceleration time interval
t_{c}	Constant speed time interval
t_{d}	Deceleration time interval
t_{e}	Instantaneous electromagnetic torque
t_{period}	The time interval of one positioning cycle
t_{r}	Rest time interval
t_{α}	Acceleration/deceleration time
U_{a}	Armature voltage
U_{f}	Field voltage
U_{n}	Nominal voltage
$\boldsymbol{u}_{\text{s}}$	Stator voltage space vector
α_{Mmax}	Motor maximum acceleration
ω_{Mmax}	Load maximum angular velocity referred to motor side
ω_{m}	Rotor angular velocity
ω_{max}	Load maximum angular velocity
ω_{L}	Angular velocity of the load shaft
θ_{r}	Rotor angle
θ_{max}	Maximum movable angle
θ_{delay}	The stop angle (stop delay)
ψ_{F}	The rotor flux in the rotor reference frame
β	Torque angle
γ	Half-angular magnetic width of PMSM
η	Efficiency
σ	Total leakage coefficient of induction machine
τ	Mechanical time constant
ξ	Damping constant
$\boldsymbol{\psi}_{\text{r}}$	Rotor flux linkage space vector
$\boldsymbol{\psi}_{\text{s}}$	Stator flux linkage space vector

ABBREVIATIONS

ac	Alternating cuurent
Acc.	Acceleration
BdcM	Brushless dc Machine
CdcM	Conventional dc machine
dc	Direct Current
DdcM	Disc armature dc Machine
Dec.	Deceleration
DTC	Direct Torque Control
IGBT	Insulated Gate Bipolar Transistor
IM	Induction Machine
NdFeB	Neodymium-iron-boron
PM	Permanent Magnet
PMSM	Permanent Magnet Synchronous Machine
PT	Phototransistor
RSM	Reluctance Synchronous Machine
SmCo	Samarium-cobalt
TIDE	European Union's funding initiative
Tr	Transistor
VC	Vector Control

ACKNOWLEDGMENTS

This work was conducted in the Department of Electrical Engineering at Lappeenranta University of Technology; it was completed with the friendly support, help, and encouragement of several persons and colleagues.

First of all, I would like to express my gratitude to Professor Juha Pyrhönen for supervising this thesis. His inspiration and support during every phase of this work has been crucial to its success.

I would also like to express my sincere thanks particularly to M.Sc. Mrs. Pia Salminen and Lic.Sc. Mr. Panu Kurronen for their continuous help and support. Your contributions and advice are deeply indebted.

I am also indebted to Mr. Jussi Salo, he helped preparing my work desk, Mr. Markku Niemelä, Tapani Manula and Harri Loisa for their help during the drive test, Mr. Sami Virtanen and Asko Salminen of ABB for their support and patience.

My thanks are also extended to everybody who helped me during this work; your cooperation and support made the writing of this thesis an enjoyable undertaking.

Sami Halabeya

TABLE OF CONTENTS

1. INTRODUCTION

1.1 General Introduction

Active biomechanical test and training systems are nowadays considered to be powerful tools for the analysis and evaluation of human musculoskeletal performance. Through multi-joint testing they can be used to assess or rehabilitate most major body joints, including the ankles, knees, hips, shoulders, elbows or wrists, in a variety of movement patterns. These biomechanical test and training systems are based on high performance industrial robot technology with fully digitally controlled drive systems.

The possible role of robotics in the field of rehabilitation has been widely investigated in the last decades. Possible specific application areas which have been already identified range from the assistance to the disabled and the elderly, by means of robotic manipulators, intelligent wheelchairs and dedicated interfaces for households and vocational devices, through the restoration of impaired functions, by means of advanced prostheses, ortheses, and electrical functional stimulation, to the development of virtual environments for training and genuine rehabilitative therapies. [21]

European research and development in the field of rehabilitation robotics was established in the mid-1970's with the Spartacus and Heidelberg manipulator projects. Since then, activities have been confined to a few well-funded research and development projects, supplemented by several smaller university-based research projects. The availability of a low cost commercial robotic arm with which to conduct research has been significant in this respect.

More recently, the European Union's TIDE funding initiative has provided an opportunity for several strands of research and development to come together in a coherent manner. TIDE was set up as a pre-competitive technology research

and development initiative specifically aimed at stimulating the creation of a single market in rehabilitation technology in Europe [23].

Nowadays, through the use of biomechanical test and training systems, it's not only possible to rehabilitate diseased people faster and bring them back to normal, but also with appropriate tests and measurements, it's even possible to avoid deficiencies in the musculoskeletal system.

1.2 Objective

The primary goal of this thesis is to design and build a three-phase variable-speed electrical motor drive system for a biomechanical testing and training equipment used mainly for musculoskeletal testing, rehabilitation, and exercise purposes.

In an older version of this equipment, a dynamometer employing a linear electromagnetic actuation, incorporating a passive non-motorized resistive braking mechanism was used to perform simple rehabilitation and training functions. The brake mechanism is inflexible and in some cases cannot actively monitor the patient performance during vital rehabilitation exercises, and consequently, fails to achieve the sought assessment.

Moreover, the recent advances in the field of rehabilitation clinics, and the increased demands for more sophisticated and intelligent rehabilitation equipment, along with a parallel advances in the field of variable-speed electrical drives that highly reduced their costs, enabled a reasonable thinking toward replacing the old passive system with a new active (motorized) one. Hence, the goal of this thesis can be stated again as designing and building a modern three-phase variable-speed electrical drive system that replaces the passive brake mechanism and achieves more flexible and powerful rehabilitation equipment.

1.3 Provision

The nature of this medical equipment and its direct interaction with humans necessitates equipment with a high level of safety, intelligence, and accuracy, while on the same time still affordable. To address such high demands, a careful selection of the drive technology should be experienced.

This work will be, therefore, divided into two major parts. The first part is devoted to studying the performance properties and control schemes of different solutions (motors) available in the electrical drives market, in order to assists in

the process of selecting the appropriate drive technology that meets such a demanding application. Modern induction motor drive is perhaps the only candidate solution to meet such demands of high performance and low price. Hence, other solutions available will be studied with respect to this machine.

The second part will focus on the drive design and testing. In this part, a complete discussion concerning the design of the selected drive, its components, simulation, worst case duty cycle, and test results is given.

2. INDUCTION MACHINE AND ITS COMPETITORS

2.1 Introduction

In the past, dc motors were used extensively in areas where variable-speed operation was required, since their flux and torque could be controlled easily by directly controlling the field and armature current. In particular, the separately excited dc motor has been used mainly for applications where there was a requirement of fast torque response and four-quadrant operation with high performance near zero speed.

However, dc motors have certain disadvantages, which are due to the existence of the commutator and the brushes. That is, they require periodic maintenance; they cannot be used in explosive or corrosive environments and they have limited commutator capability under high-speed, high-voltage operational conditions. These problems can be overcome by the application of alternating current (ac) motors, which can have simple and rugged structure, high reliability and economy; they are also robust and immune to heavy overloading. Their small dimension compared with dc motors allows ac motors to be designed with substantially higher output ratings for low weight and low rotor inertia. [1]

Variable-speed ac drives have been used in the past to perform relatively undemanding roles in applications which preclude the use of dc motors, either because of the working environment or commutator limits. The inability of ac drives -despite the ac motor excellent properties- to compete with dc drives in variable-speed applications was mainly due to the difficulty in controlling the ac motor flux and torque. A high cost, efficient and fast switching frequency converters were needed to achieve a satisfactorily ac machine control. As a result of the progress in the field of power electronics, with the continuing trend towards cheaper and more effective power converters, variable-speed ac drives today are able to compete favorably on a purely economic basis with dc drives.

Among the various ac drive systems, those that contain the squirrel-cage induction motor have a particular cost advantage. The squirrel-cage induction motor is simple and rugged and one of the cheapest machines available at all power ratings. Owing to their excellent control capabilities, variable-speed drives incorporating squirrel-cage induction motors and employing modern static converters and direct torque control can well compete with high-performance four-quadrant dc drives.

This chapter will focus on the modern and most efficient control schemes applied to ac machines. The control schemes that are the subject of this text are studied with respect to induction machine; due to the widespreadness of this machine in various applications and the importance it has in the field of ac drives from many aspects. This of course does not deny the extension of the same control concepts to other ac machines. In fact, these control approaches can be applied to any ac machine on the same basis; therefore, the control schemes of other ac machines described in this chapter are not given individually.

Before studying induction machine and its control schemes, it's useful (for the sake of comparison) to start with a look at the control schemes and practical performances of the main competitors to induction machine available in the electrical drives market.

One of the main competitors to induction machine in a very wide range of applications is the dc machine introduced in the next section. Among the others, Permanent Magnet Synchronous Machine (PMSM) and Reluctance Synchronous Machine (RSM) have become increasingly attractive for many applications, particularly following the introduction of neodymium-iron-boron and samarium-cobalt magnetic materials, and a more reliable RSM rotor constructions.

2.2 Direct-Current (dc) Machine

Direct-current machines are characterized by their versatility. By means of various combinations, shunt, series, and separately excited field windings they can be designed to display a wide variety of volt-ampere or speed-torque characteristics for both dynamic and steady state operations.

Because of the ease with which they can be controlled, systems of dc machines are often used in applications requiring a wide range of motor speed or precise control of motor torque.

2.2.1 Conventional (Brush) dc Machine

A conventional dc machine consists of a stationary field structure utilizing a stationary dc excited winding or permanent magnets and a rotating armature (rotor) winding supplied through a commutator and brushes. This basic structure is schematically illustrated in Figure (2.1) along with the resulting orientation of the armature mmf (I_a) and the field flux.

The action of the commutator is to reverse the direction of the armature winding currents as the coils pass the brush position such that the armature current distribution is fixed in space no matter what rotor speed exists.

The function of the compensating windings shown in the figure is to maximize the machine torque and simplify its control by ensuring an angle of 90° between the field flux and armature mmf.

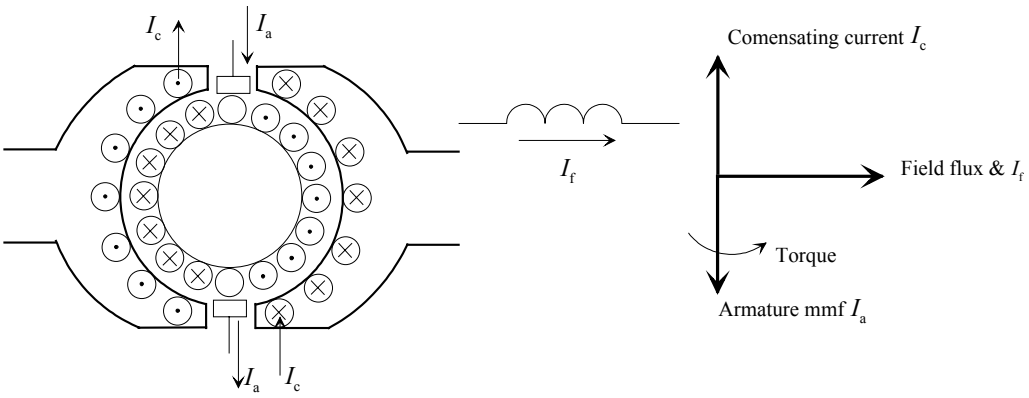

Figure 2.1. Orientation of armature mmf and field flux of a fully compensated dc machine. [2]

As shown in Figure (2.1), the field flux and armature mmf are maintained in a mutually perpendicular orientation independent of rotor speed. The result of this orthogonality is that the field flux is unaffected by the armature current and both of them can be controlled independently.

The electromagnetic interaction between the field flux and the armature mmf results in two basic outputs, an induced voltage proportional to rotor speed, and an electromagnetic torque proportional to the armature current [Equations (2.1) and (2.2), respectively].

$$E_a = k_\phi \, \omega_m \tag{2.1}$$

$$T_e = k_\phi \, I_a \tag{2.2}$$

By assuming $k_\phi = \frac{p}{2}\psi_f$ to be constant, and ω_m the rotor angular velocity. The simplicity of the model is strongly dependent on the mutually perpendicular orientation of the flux and mmf. If this orthogonality were disturbed two major complications occur, firstly, the field flux is no longer independent of the armature current since there will be an mmf component in the field axis. Secondly the torque relation [Equation (2.2)] will be modified by the addition of

an angle dependent function (phase) which will result in a complexity of machine control similar to that of induction machine.

Adjustable speed operation is normally attained by operating with a fixed field flux while varying the armature voltage [*see* Equation (2.1)]. Torque production requires armature current and results in armature voltage drop through the motor armature resistance (R_a). This voltage drop must come at the expense of a smaller induced voltage, which necessitates a small speed reduction. Thus, every armature voltage has an associated torque speed curve and the actual speed of operation is determined by the armature voltage and the torque required to supply the load.

Adjustable torque operation is readily attainable in the dc machine by the simple action of controlling the armature current instead of voltage. As expressed in Equation (2.2), with a constant value of the flux, the torque is directly proportional to armature current. Thus the torque can be adjusted as accurately and rapidly as the armature current can be adjusted and controlled. In practice this is accomplished by using a feedback current regulator and a power electronic supply. If both positive and negative values of torque and speed are required, the supply must be capable of bi-directional current and voltage. Very rapid current changes require large transient armature voltage to overcome the inductive effects, and operation at high speed requires a large average voltage to supply the speed dependent induced voltage [*see* Figure (2.2) and Equation (2.3)].

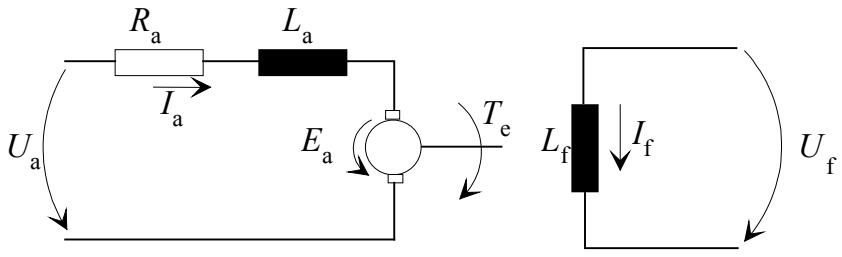

Figure 2.2. Equivalent circuit of a separately excited dc machine. [2]

$$U_{\mathrm{a}} = E_{\mathrm{a}} + I_{\mathrm{a}} R_{\mathrm{a}} + L_{\mathrm{a}} \left(\frac{\mathrm{d}\, I_{\mathrm{a}}}{\mathrm{d}\, t}\right) \qquad (2.3)$$

However, the torque will exactly follow the current and to the extent that the current regulator follows its reference input, the torque will be proportional to the current reference of the regulator. Figure (2.3) illustrates the elements of a typical torque controlled dc motor drive.

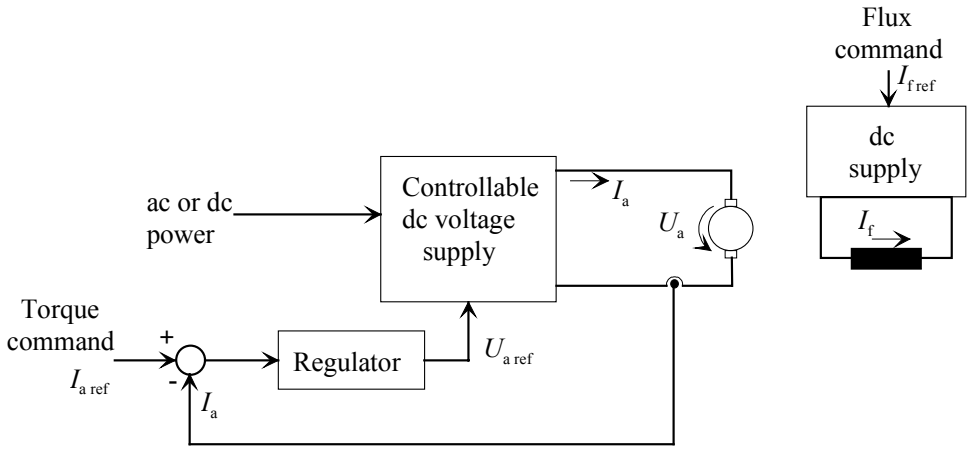

Figure 2.3. Elements of a torque controlled separately excited dc motor drive.

Following the concepts outlined for the dc machine, it is noted that a simple and efficient torque control of any machine can be achieved if the following requirements are met:

a) an independently controlled armature current, and
b) an independently controlled or constant value of the flux, and
c) an independently controlled orthogonal spatial angle between the flux axis and the mmf axis to avoid any interaction between them. [2]

In dc machines, requirements (b) and (c) are assured by the commutator and the separate field excitation system (dc winding or permanent magnet). In ac machines, these requirements must be achieved by external controls and thus the situation is more complex.

Practical Performance

The dynamic response of the dc machine is an important factor in variable-speed applications (e.g. servo-drives). If in some cases, rapid acceleration of a high inertia rotating system is required, the motor maybe required to develop a torque at low speed, well in excess of the eventual steady load torque. The use of conventional dc machines in such cases is limited by its relatively heavy rotor with high moment of inertia and its long mechanical time constant.

As some part of the motor torque is spent generally on accelerating the motor inertia, the latter should be made as small as possible to increase the amount of motor torque available for accelerating the load.

$$T_m = T_{inertia} + T_L \tag{2.4}$$

Brushed non-conventional dc machines with high dynamic response, and high torque to inertia ratios were constructed to replace conventional (brush) dc machines in high performance drives. Such machines are called moving-coil machines, since they do not have an iron core (coreless) in their rotor. An example of a moving-coil machine is the axial air-gap motor with a disk armature structure (printed-circuit armature, pancake…).

In such machine, the magnetic field is axially directed rather than radially as the case in their conventional counterparts, leading to a very compact motor. Permanent magnets on the machine stator provides an axial excitation magnetic flux that interacts with the armature winding (formed on e.g. a printed circuit board) to produce torque.

Catalogue data for conventional brush type dc machine designed for high performance dc servo drives versus disc armature dc machine is given in Table (2.1), both machines are provided by PARVEX servo systems.

Table 2.1. Catalogue data for conventional versus disc armature dc machines.

Manufacturer		PARVEX servo systems [3]			PARVEX servo systems [4]		
Property	Symbol	Conventional (iron core)			Disc armature (coreless)		
		T4F1B	T5F4B	T7F3B	F12M4H	MC23S	MC27
Rated torque	T_n (Nm)	1.2	8	25	1.1	7	22.9
Rated speed	n_n (rpm)	3050	2600	2300	3000	3000	3000
Rated current	I_n (A)	2.8	14.9	40	7.2	14.8	52
Rated voltage	U_n (V)	170	170	170	61	172	154
Inertia	J (kgcm^2)	11	71	460	1.6	23	74
Torque/inertia	Nmkg^{-1}m^{-2}	1091	1127	543.5	6875	3043.5	3094.6
Mechanical time constant	τ (ms)	26.1	10.6	11	4.7	8	6
Mass	m (kg)	8	23	44	5	17	35

The torque/inertia ratios of a disc armature dc machine are more than five times [Table (2.1)] higher than their conventional counterparts. It's also evident that the disc armature dc machine has lower mechanical time constants, which means faster dynamic response.

2.2.2 Brushless dc Machine

Conventional dc machines are -as stated above- efficient and easy to control, however, the presence of the mechanical commutator and brushes which are subjected to wear and require periodic maintenance, causes a significant reduction in machine reliability.

When the functions of commutator and brushes were implemented by solid-state switches, maintenance-free motors were realized. These motors are known as brushless dc motors. In conventional dc motors, the armature is the rotor, and the field windings (or magnets) are placed in the stator. A brushless dc motor of this structure is very difficult to make. The construction of a modern brushless dc motor is very similar to the permanent magnet synchronous ac motor; the armature windings are part of the stator and the rotor is composed of one or more magnets. The windings of a brushless dc motor are similar to those used in polyphase ac motors and the most efficient motor has a set of three-phase windings and is operated in bipolar excitation as illustrated in Figure (2.4) below.

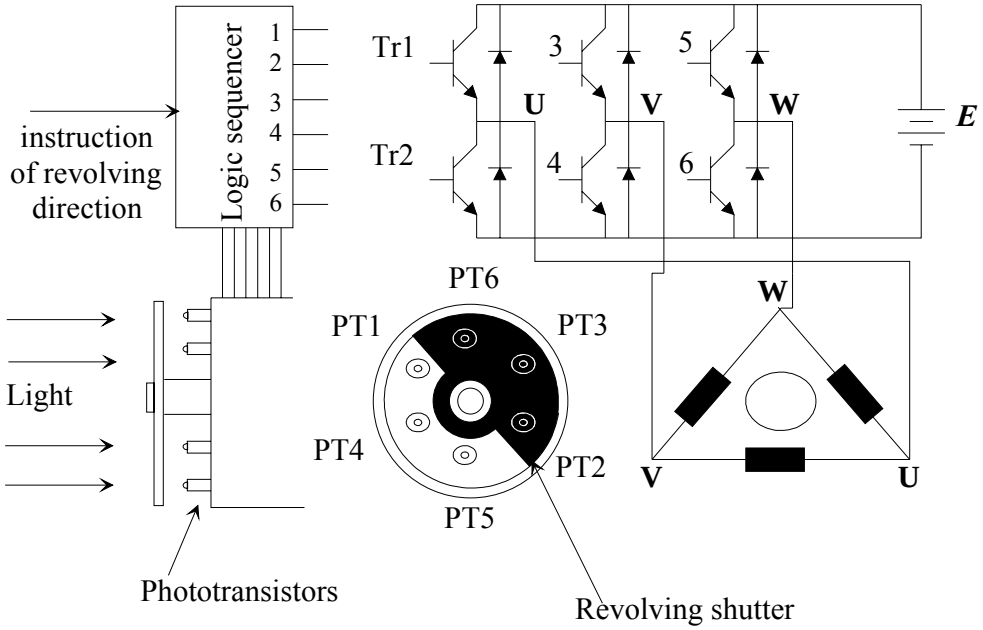

Figure 2.4. Three-phase bipolar-driven brushless dc motor. [5]

Hall elements or optical sensors (e.g. phototransistors as in the above figure) are used to detect the rotor position. When a three-phase brushless motor is driven by a three-phase bridge circuit, the efficiency is the highest, since in this drive an alternating current flows through each winding as in an ac machine. A drive of this type is often referred to as a bipolar drive, which means that a winding is alternatively energized in the south or north poles giving the ability to reverse the rotational direction of the motor.

In Figure (2.4), six phototransistors are placed to the end plate at equal intervals. Since a shutter is coupled to the shaft, these photo elements are exposed in sequence to the light emitted from a lamp placed in the left of the figure. The simplest relation between the ON/OFF of the transistors and the light detecting phototransistors is set when the logic sequencer (shown) is arranged in such a way that when a phototransistor marked with a certain number is exposed to light, the transistor of the same number turns on. Therefore, the state shown in Figure (2.4) indicates that electrical currents flow through Tr1, Tr4, and Tr5, and

terminals U and W have the battery voltage, while terminal V has zero potential. In this state a current will flow from terminal U to V, and another current from W to V as illustrated in Figure (2.5). The thin arrows in the figure indicate the directions of the magnetic fields generated by current in each phase, while the solid arrow in the center is the resultant magnetic field in the stator.

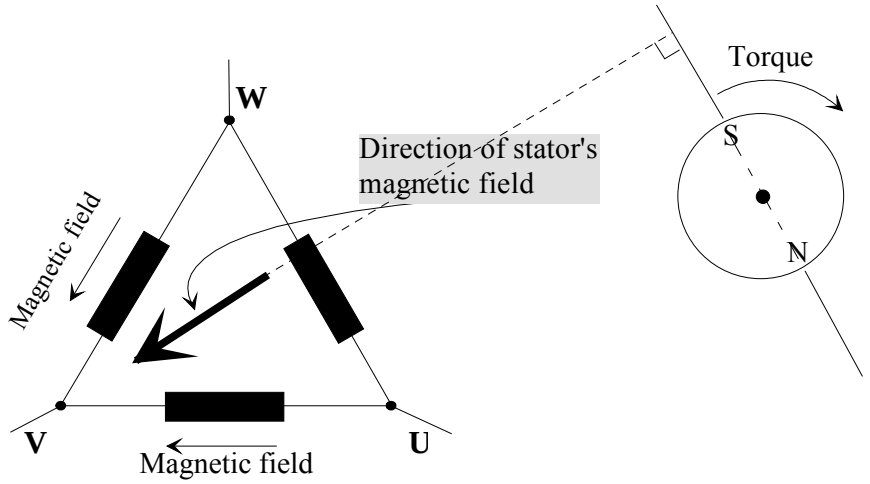

Figure 2.5. Stator's magnetic field in the shutter state of Figure (2.4), and the direction of torque. [5]

In such a state a clockwise torque will be produced on the rotor. After it revolves through about 30°, PT5 is turned OFF and PT6 is turned ON which makes the stator magnetic pole revolve 60° clockwise. Thus when the rotors south pole gets near, the stator south pole goes away further to create a continuous clockwise rotation. The rotational direction may be reversed by reversing the switching logic of the transistors.

An important feature that highly simplifies the motor's control, is the rotor orientation with respect to stator (armature) magnetic field, i.e. they are spaced 90° from each other as illustrated in Figure (2.5). In other words, the required orthogonality [mentioned in section (2.2.1)] between the motor flux-axis and its mmf-axis is maintained in brushless dc motors, and therefore, brushless dc motor will have a simple and direct flux and torque control (comparable to that of a

conventional dc machine). Thus machine torque can be written in accordance with Equation (2.2) as:

$$T_e = k_\varphi \hat{I}_s \tag{2.5}$$

Where $\hat{I}_s$ is the amplitude of the stator current [5]. Brushless dc motor is field oriented in the sense that the field flux and armature mmf are held to a fixed relative spatial position, hence, vector control can be employed to control them.

The major disadvantage of brushless dc motor drives is their relatively high cost, a reason why, modern variable-speed induction motor drives (utilizing innovative low cost controllers) is considered to be a more economic alternative.

Practical Performance

Brushless dc machines for high performance applications are available in various constructions. The absence of commutator and brushgear reduces the motor rotor inertia; thus, high torque/inertia ratios are achievable.

The use of high performance magnetic materials like Samarium-cobalt (SmCo) or Neodymium-iron-boron (NdFeB) enables a high peak torque to stall torque ratio. Special construction techniques for mounting the permanent magnets on the rotor surface results in relatively low rotor inertia, and thus, higher dynamic performance than that of conventional dc machines.

Table (2.2) below gives practical catalogue data for two types of PM brushless dc machines with comparable ratings, one using SmCo and the other NdFeB permanent magnet materials both mounted on the rotor surface.

Table 2.2. Catalogue data for two types of PM brushless dc machines.

Manufacturer		SEM Ltd. [6]		Kollmorgen Seidel GmbH & Co. [7]
Type of PM		SmCo		NdFeB
Property	Symbol			
		HD115C6-44	HD70C4-44	BH-124-B
Rated torque	T_n (Nm)	6.8	1.2	1.3
Rated speed	n_n (rpm)	6000	8000	6000
Rated current	I_n (A)	13.2	2.3	1.8
Rated voltage	U_n (V)	260	350	400
Inertia	J (kgcm^2)	4.6	0.6	0.46
Torque/inertia	Nmkg^{-1}m^{-2}	14782.6	20000	28260
Mechanical time constant	τ (ms)		1.6	
Mass	m (kg)	9	2.6	3.2

While both machines are having a relatively very high dynamic performance, the machine with NdFeB permanent magnet material has a superior performance over that with SmCo material. From Table (2.2), the HD70C4-44 machine has rotor inertia of 0.6, while the BH-124-B machine (with NdFeB permanent magnet material) has rotor inertia of only 0.46. Which means over 23 % reduction of rotor inertia is achievable with the NdFeB PM machine, while in the same time its rated torque (1.3 Nm) is still higher than that of the SmCo PM machine (1.2 Nm). Thus, a further increase in machine dynamic performance is obtained by using the new high performance permanent magnet material NdFeB.

The brushless PM dc machine has much higher dynamic performance than its conventional (brushed) type. This becomes obvious if a simple comparison is made between the machine T4F1B in Table (2.1) and the machine BH-124-B in Table (2.2). With the latter its possible to achieve a higher rated torque (1.3 Nm) than the former (1.2 Nm), provided that, a reduction of more than 95% of the rotor inertia is obtained. PM excitation is viable only for smaller motors, usually below 20 kW, since for higher rates the price of the permanent magnet materials becomes excessive, therefore, other machine types are used for ratings beyond that (e.g. induction machines).

2.3 Permanent Magnet Synchronous Machine (PMSM)

As pointed out by its name, permanent magnet synchronous machines uses permanent magnets to produce the required air-gap magnetic flux rather than field coils as in traditional synchronous and dc machines. Significant advantages arise from the reduction in losses and improvement in efficiency.

A PMSM is made in a number of configurations; one of the simplest is shown in cross section in Figure (2.6). Small motors typically have this two-pole construction, larger ratings, however, uses four or more poles. The rotor has an iron core which maybe solid or made of punched laminations, thin permanent magnets are mounted on the surface of this core. The stator contains a three-phase distributed winding, similar to that of induction machine. The rotor magnets of opposite directions produce a radially directed flux density across the air-gap, which then reacts with currents in the three-phase stator windings to produce torque.

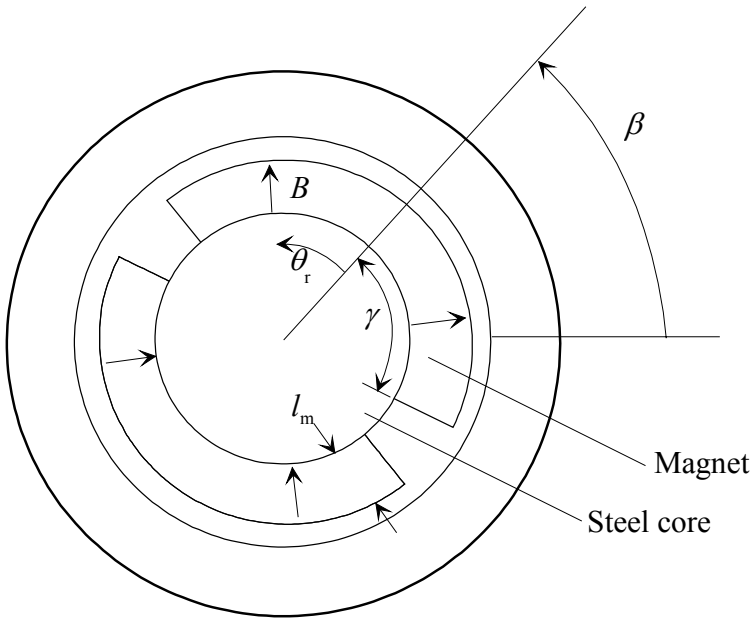

Figure 2.6. A cross section view of a two-pole PMSM. [21]

A review of the characteristics of permanent magnet materials provides a basis for appreciating the potential and limitations of PMSM. Magnetization characteristics of the most common magnetic materials currently used in motors are shown in Figure (2.7).

All of these permanent magnetic materials have their magnetic domains well aligned resulting in an essentially straight-line (linear) relationship in much if not all of the second quadrant of the *B*-*H* loop.

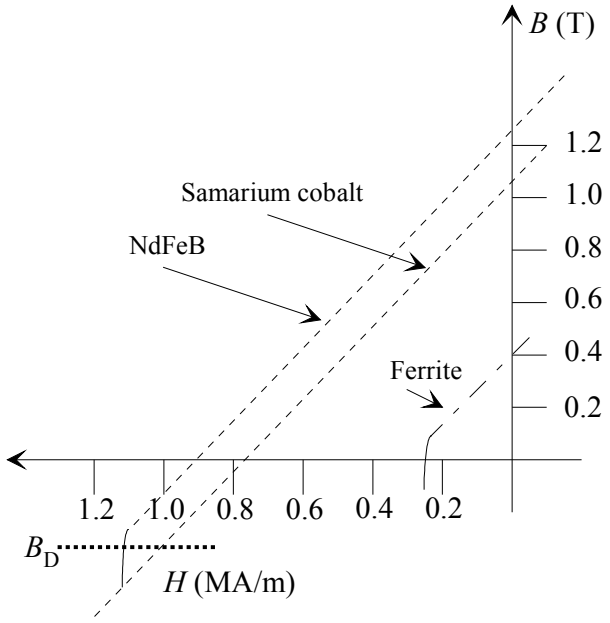

Figure 2.7. *B*-*H* characteristics for some permanent magnet materials. [8]

The slope of this characteristic is such that the magnet looks like a constant current source encircling a block of material with relative permeability just greater than air, i.e. $\mu_r \approx 1.05\text{-}1.07$. The magnet can be operated at any point on the linear part of the *B*-*H* characteristic and remain permanent. However, if the flux density is reduced beyond the knee of the characteristic (denoted as flux density B_D) some magnetism will be lost permanently. On removal of a demagnetizing field greater than this limit, the new characteristic will be a straight line parallel to but lower than the original.

2.3.1 Types of Permanent Magnet Materials

A close look at the properties of the permanent magnetic materials shown in Figure (2.7) is given below. The performance of PMSM depends greatly on the magnetic properties of the permanent magnet material used.

Ferrite Permanent Magnet Material

Ferrite permanent magnet materials have been available for decades, their cost is attractively low, however, their residual flux density at only 0.3-0.4 T is very low. Simultaneously, ferrites, which are made with a higher residual flux density, also have a higher value of B_D and thus are more easily demagnetized.

Ferrites have high resistivity and thus have low core losses in situations with rapidly varying flux components. Ferrites can be operated at temperatures up to 100°C, increase in temperature increases the residual flux density and decreases the knee point density B_D. At very low operating temperatures, special care is needed to ensure that demagnetization does not occur.

Samarium Cobalt Permanent Magnet Material

Samarium cobalt magnets have a higher value of magnetic flux density (0.8-1.1 T). They are highly resistant to demagnetization having values of B_D well into the third quadrant of the *B-H* loop. The residual flux density decreases somewhat with increase in temperature while the knee point density B_D increases, signifying an increased sensitivity to demagnetization as temperature is increased. The cost of these materials is relatively high compared to ferrites. The resistivity is about 50 times that of copper.

Neodymium-iron-boron (NdFeB) Permanent Magnet Material

The introduction of NdFeB materials in 1983 provided a major impetus to the use of permanent magnets in motors. At room temperature, the residual flux density of NdFeB is in the range 1.1-1.25 T. This is adequate to produce a flux density of

0.8-0.9 across a relatively large air-gap, e.g., 1mm with a magnet thickness of only about 3-4 mm. The residual flux density reduce by about 0.1% for each degree rise in temperature. The knee point flux density B_D increases rapidly with temperature imposing a limit on the maximum operating temperature of NdFeB in the range 100-140°C depending on the detailed structure. The resistivity is about 85 that of copper.

The cost of NdFeB material is still relatively high, largely because of manufacturing complexity of the mill-and-sinter process. It is expected that the cost of this material will drop in the future, since two of the basic materials iron (77%) and boron (8%) cost relatively little and neodymium is one of the common rare-earth elements [8].

2.3.2 Torque Production

The stator of PMSM as shown in Figure (2.6) is identical to that of an induction machine. The three-phase stator windings are each distributed to provide a sinusoidal distribution of linear current density around the air-gap periphery so that a set of phase currents, sinusoidally varying with time, will set up a field that is also sinusoidally distributed peripherally and is rotating at synchronous speed.

The air-gap flux density B_g maybe approximated by

$$B_g \approx B_r \frac{l_m}{l_g} \quad \text{T} \tag{2.6}$$

where l_m is the magnet thickness and l_g is the air-gap length. The flux density produced by the magnets is a rectangularly distributed wave of relatively constant magnitude and of alternating polarity. To the extent that the stator windings are approximately sinusoidally distributed, only the fundamental space component of the magnetic flux density wave can link with the stator windings. The magnitude of this component is directly proportional to sin (γ), where γ is the

half-angular width of the magnet [*see* Figure (2.6)]. When the rotor of the machine rotates with speed n_m, the effect of the rotor as seen by the stator can be represented as a sinusoidal current source of constant magnitude. The angle β shown in Figure (2.6) is the electrical angle between the stator current space vector and the rotor magnetic flux, which in turn is related directly to the angular position of the rotor. The instantaneous torque of a three-phase PMSM can be expressed as:

$$t_e = 3\frac{p}{2}\psi_F i_{sq} \tag{2.7}$$

where ψ_F is the rotor flux in the rotor reference frame and i_{sq} is the torque-producing stator current component in the rotor reference frame, and p is the number of machine pole-pairs. The torque of the PMSM is a maximum when the torque angle β is 90°, and it varies with the sine of β.

Practical Performance

Sample practical catalogue data of PMSM is shown in Table (2.3) below. The magnetic material used is NdFeB, leading to a high performance machine.

Table 2.3. Catalogue data for two PMSM's using NdFeB magnetic material.

Manufacturer		ABB [9]		Kollmorgen Seidel GmbH & Co. [10]
Type of PM		NdFeB		NdFeB
Property	Symbol			
		8C1.1.30	8C4.1.30	SM100S-1.200
Rated torque	T_n (Nm)	1.3	7.5	36
Rated speed	n_n (rpm)	3000	3000	1200
Rated current	I_n (A)	1.4	4.7	31
Rated voltage	U_n (V)			
Inertia	J (kgcm^2)	0.9	9.4	108
Torque/inertia	Nmkg^{-1}m^{-2}	14444.4	7978.7	3333.3
Mass	m (kg)	3.1	9	32.7

At least for the machines described in this paper, the brushless PM dc machine has a much better dynamic performance than the PMSM. This can be seen by comparing the BH-124-B brushless PM dc machines given in Table (2.2) with the PMSM 8C1.1.30 given in Table (2.3), as they both have comparable torque ratings. The rotor inertia of the brushless PM dc machine (BH-124-B) is about 49% less than that of the PMSM, thus, the brushless PM dc machine is expected to achieve higher acceleration values than the PMSM.

2.4 Reluctance Synchronous Machine (RSM)

An RSM is a salient pole synchronous machine, its stator is identical to that of induction or synchronous machine. However, its rotor is a salient-pole one, therefore, its torque production follows the principle of reluctance torque.

In earlier constructions, rotor saliency was achieved by removing certain teeth from the rotor of a conventional squirrel-cage. Such machines have been used for a long time and their inferior performance and relatively high price have resulted in a limited use. However, as a result of recent developments, more reliable and robust new constructions exists, these have basically three types of rotors: segmental, flux barrier, and axially laminated rotors.

2.4.1 Torque Production

The stator of RSM contains three-phase excitation windings where a three-phase set of sinusoidal stator currents are running, which produces a sinusoidally distributed rotating field in the machine air-gap. As the rotor is shaped with a small air-gap in the direct axis (*d*-axis) and a large air-gap in the quadrature axis (*q*-axis), the magnetizing inductance changes going through maxima and minima as it rotates synchronously. Thus, the torque of this motor can be expressed as:

$$t_e = 3\frac{p}{2} L_{sd}\left(1 - \frac{L_{sq}}{L_{sd}}\right) i_{sd} . i_{sq} \tag{2.8}$$

and the maximum power factor of the machine is

$$\cos\varphi_{max} = \frac{L_{sd}/L_{sq} - 1}{L_{sd}/L_{sq} + 1} \tag{2.9}$$

Equation (2.9) clearly shows that the maximum power factor of the RSM is completely dependent upon the ratio (L_{sd}/L_{sq}), this ratio is an RSM important design parameter, usually it is referred to as the saliency ratio.

From Equations (2.8) and (2.9), it is seen that in order to maximize the motor torque and power factor, the rotor saliency ratio should be made as high as possible. In the RSM with segmental rotor, saliency ratios of 6-7 have been obtained. If the number of rotor segments is very large, then a distributed anisotropic structure is obtained, by using multiple segmental structures, the saliency ratio can be increased.

In a high performance RSM the rotor is axially laminated, this results in a high saliency ratios (up to 12 has been obtained) [8]. The high saliency ratio results in high power density, increased torque, high power factor, and increased efficiency.

Practical Performance

Extensive efforts and studies have been continuously carried out lately aiming towards performance enhancement of the reluctance synchronous machine. Much of the efforts are spent upon improving the machine rotor construction to achieve as high saliency ratio as possible (e.g. using different construction approaches). As this machine is still under extensive study, only prototype motor data is shown here. Table (2.4) below gives practical data for two prototype reluctance synchronous motors.

Table 2.4. Prototype data for tow high performance RSM's.

Property	Symbol		
		Prototype 1 [11]	Prototype 2 [12]
Rated torque	T_n (Nm)	7.5	18
Rated speed	n_n (rpm)	1500	6685
Rated current	I_n (A)	20	11.6
Rated voltage	U_n (V)	350	440
Inertia	J (kgcm^2)	100	30
Torque/inertia	Nmkg^{-1}m^{-2}	750	6000

2.5 Induction Machine

Induction machines have been used for more than a century. Because of their simplicity, ruggedness, reliability, and low cost induction machines with squirrel-cage rotor are the most commonly used machines at fixed-speed. However, due to the recent development in the field of variable-speed drives, they are now finding increasing acceptance in various industrial variable-speed applications historically restricted to dc machines.

The name induction machine comes from the fact that the rotor of induction machine receives its power by induction (not direct conduction as in a dc machine). A winding that receives its power exclusively by induction constitutes a transformer. Therefore, an induction machine is a transformer with a rotating secondary winding and its steady-state equivalent circuit is identical to that of a transformer.

There are two basic types of induction machines: single-phase and polyphase machines. Single-phase induction machines are favored for domestic applications. A large number of these machines are built in the fractional horsepower range. On the other hand, polyphase induction machines cover the entire spectrum of horsepower rating. Owing to the widespread generation and transmission of three-phase power, most polyphase induction machines are of the three-phase type.

The stator of induction machine is of conventional type, identical coils are wound into its slots, and these coils are then connected to form a balanced three-phase winding used to excite the machine. The rotor of induction machine is constructed in different forms, the most common form is known as the squirrel-cage rotor. Its core is made of a stack of sheet-steel laminations. Aluminum, copper, or bronze conductors are placed in slots around the outer periphery of the rotor core, these conductors are then shorted together by circular end rings at each end of the rotor.

In most rotors, the slots are not parallel to the axis but are skewed in an angle, this is done to avoid a cogging torque which might otherwise arise due to a varying ferromagnetic attraction force between rotor teeth and stator teeth as the rotor rotates.

2.5.1 Principle of Operation

When the stator winding of a three-phase induction machine is connected to a three-phase power source, it produces a magnetic field that is constant in magnitude and revolves around the periphery of the rotor at synchronous speed.

If f is the frequency of the current in the stator winding and p is the number of the machine pole-pairs, the synchronous speed of the revolving field is:

$$n_s = \frac{60\,f}{p} \tag{2.10}$$

The revolving field induces electromagnetic force (emf) in the rotor winding. Since the rotor winding forms a closed loop (short circuited by the end rings), the induced emf in each coil gives rise to an induced current in that coil. When a current carrying coil is immersed in a magnetic field, it experiences a force (or torque) that tends to rotate it. The force developed and thereby the rotation of the rotor are in the same direction as the revolving field.

Under no load, the rotor soon achieves a speed nearly equal to the synchronous speed. However, the rotor can never rotate at the synchronous speed, simply because at that speed the rotor coils would appear stationary with respect to the revolving field and there would be no induced emf in them. In the absence of an induced emf in the rotor coils, there would be no current in the rotor conductors and consequently no force would be experienced by them. In the absence of a force, the rotor would tend to slow down. As soon as the rotor slows down, the induction process takes over again.

In summery, the rotor receives its power by induction only when there is a relative motion between the rotor speed and the revolving field. If n_m is the rotor speed at a certain load, the relative speed of the rotor with respect to the synchronous speed of the revolving filed is

$$n_r = n_s - n_m \tag{2.11}$$

This relative speed is also called the slip speed. This is the speed with which the rotor is slipping behind the synchronous speed. However, it is a common practice to express the slip speed in terms of the slip (*s*), which is a ratio of the slip speed to the synchronous speed (slip on a per unit basis). That is,

$$s = \frac{n_r}{n_s} = \frac{n_s - n_m}{n_s} \tag{2.12}$$

The slip can also be expressed as a percentage of the synchronous speed (percent slip). Thus, the rotor speed can be written as:

$$n_m = (1 - s)\, n_s \tag{2.13}$$

When the rotor is stationary, the per-unit slip is 1, the frequency of the induced emf in the rotor winding is the same as that of the revolving field. However, when the rotor rotates, it is the relative speed of the rotor n_r that is responsible for the induced emf in its winding, and consequently, the developed torque [13].

The instantaneous torque of induction machine can be expressed in several ways, either as the cross product of stator flux and the stator current space vectors or the rotor flux and rotor current space vectors or even as the cross product of the stator and rotor flux space vectors, which is more instructive here [14].

$$t_e = \frac{3}{2} p \frac{(1-\sigma)}{\sigma L_m} \boldsymbol{\psi}_r \times \boldsymbol{\psi}_s \tag{2.14}$$

where $\sigma = 1 - \frac{L_m^2}{L_s L_r}$ is the machine total leakage coefficient, L_m, L_s, and L_r are the machine magnetizing inductance, stator inductance and rotor inductance respectively.

Practical Performance

Induction machine has a better dynamic performance than a conventional dc machine, however, its performance lags far behind that of permanent magnet brushless dc or synchronous machine. Nevertheless, the relative low cost and availability of induction machine constructions that cover a wide power range were enough to make this machine such a strong competitor to other high performance ac and dc machines.

Table (2.5) below gives practical catalogue data for a couple of three-phase squirrel-cage induction motors.

Table 2.5. Catalogue data for four squirrel-cage induction machines.

Manufacturer		ABB [15]			Lenze[16]
Property	Symbol				
		M2AA 63B	M2AA 90S	M2AA 100 LB	MDSKA080-22.70
Rated torque	T_n (Nm)	1.25	7.5	20	6.7
Rated speed	n_n (rpm)	1370	1410	1430	2000
Rated current	I_n (A)	0.72	2.59	6.48	3.85
Rated voltage	U_n (V)	400	400	400	390
Inertia	J (kgcm^2)	2.8	32	82	19.2
Torque/inertia	Nmkg^{-1}m^{-2}	4464.3	2343.7	2439	3490
Mass	m (kg)	4.5	13	24	15.1

2.6 Performance Comparison

From the practical data -given above- for every machine studied, a measure of the dynamic performance of the machine was obtained. The dynamic performance of a machine was appreciated by its torque/inertia ratio.

In this section, a performance comparison between induction machine and other dc and ac machines described above is made based on machines practical (catalogue) data. To simplify the task of comparison, Table (2.6) below extracts the machines to be compared from the practical data tabulated above, and summarize them in a way suitable for comparison.

Table 2.6. Compared machines.

			Torque	Inertia	Torque/inertia
Machine	Name	Table	(Nm)	(kgcm^2)	Nmkg^{-1}m^{-2}
CdcM	T5F4B	2.1	8	71	1127
DdcM	MC23S	2.1	7	23	3043.5
BdcM1	BH-124-B	2.2	1.3	0.46	28260
BdcM2	HD115C6-44	2.2	6.8	4.6	14782.6
PMSM	8C4.1.30	2.3	7.5	9.4	7978.7
RSM	Prototype 2	2.4	18	30	6000
IM1	MDSKA080-22.70	2.5	6.7	19.2	3490
IM2	M2AA 63B	2.5	1.25	2.8	4464.3
IM3	M2AA 90S	2.5	7.5	32	2343.7
IM4	M2AA 100LB	2.5	20	82	2439

The performance comparison is made between machines with comparable rated torques by invoking their torque/inertia ratios; machines with higher ratios have better dynamic performance.

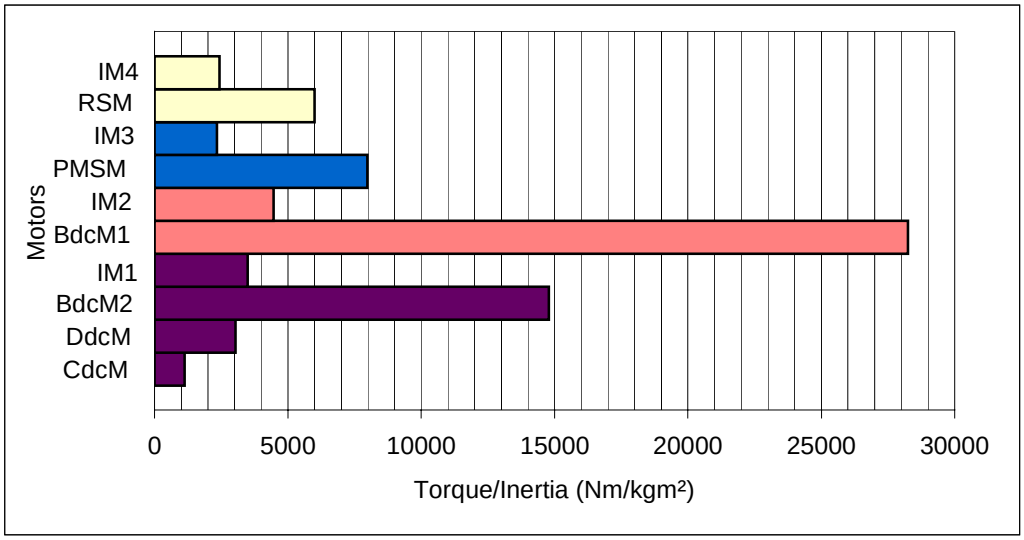

Figure 2.8. Torque/inertia ratios of the various machines compared. BdcM: Brushless dc Machine, CdcM: Conventional dc Machine, DdcM: Disc armature dc Machine, IM: Induction Machine, PMSM: Permanent Magnet Synchronous Machine, RSM: Reluctance Synchronous Machine.

The chart shown in Figure (2.8) is a graphical representation of Table (2.6); note that the machines in this chart are grouped according to their rated torque as:

Group 1: includes CdcM (Conventional dc machine), DdcM (Disc armature dc Machine), BdcM2 (Brushless dc Machine), and IM1 (Induction Machine). The machine with the highest dynamic performance is the brushless dc machine (BdcM2), it has far better dynamic performance than induction machine (IM1). It is also noted that induction machine (IM1) has a comparable dynamic performance to disc armature dc machine (DdcM) and a far better performance than conventional dc machine (CdcM).

Group 2: includes BdcM1 and IM2, this brushless dc machine (with NdFeB permanent magnetic material) has a much higher dynamic performance than

induction machine (IM2), a dynamic response of more than six times faster than induction machine (IM2) is achieved by the brushless dc machine (BdcM1).

Group 3: includes PMSM (Permanent Magnet Synchronous Machine) and IM3, it is evident that the PMSM has a higher dynamic performance than induction machine (IM3), more than three times better performance. However, the performance of PMSM is still much lower than that of a brushless dc machine [*see* section (2.3)].

Group 4: includes RSM (Reluctance Synchronous Machine) and IM4, the RSM has a surprisingly much higher dynamic performance than induction machine (IM4), although the induction machine compared (IM4) has a higher rated torque. A reduction of about 63 % of rotor inertia is achieved by RSM of the same ratings.

From the comparisons made above, it is noted that induction machine is not the best machine from the dynamic performance point of view, moreover, induction machine dynamic performance lags far behind its brushless dc, PMSM, and RSM counterparts. Nevertheless, induction machine is still one of the most commonly used machines, with applications that covers the whole power spectrum, this is due to the fact that induction machine is still one of the cheapest machines available at all power ratings.

Table (2.7) below gives the prices of three machines, conventional dc, brushless dc, and induction machine.

Table 2.7. Prices of three high performance machines.

Manufacturer	SEM Ltd. [6,17]		ABB[15]
Type	Conventional PM dc	Brushless PM dc	Induction machine
	MT 40ZD4-45	HD115 G6	M2AA 90 L
Rated torque (Nm)	11	13	10
Price (Units)	3	3.2	1

From the table above, the price of induction machine is only about one third of both conventional and brushless dc machines with the same torque ratings, the high cost of permanent magnet materials and the low production volumes are the main reasons for the high price of the dc machine as a whole.

2.7 Control Schemes of Induction Machine

Although induction machine is superior to dc machine with respect to size, weight, maximum speed and reliability, because of its highly non-linear dynamic structure with strong dynamic interactions, it requires much more complex control schemes than those discussed above (for dc machines).

The complexity of controlling induction machines arises from the presence of rotor slip; the revolving stator magnetic field is not stationary with respect to armature mmf or rotor magnetic field (as in dc machines), but there is a slip speed between them given by Equation (2.11). This implies that the orthogonality relation between the directions of the field flux and the armature mmf is no longer maintained and a component of the mmf in the direction of the field flux will exist. Therefore, to effectively control the machine, any control scheme proposed (e.g. external) should tend to retain the required orthogonality relation mentioned above.

In fact modeling of induction machines using space vector theory has revealed that the mechanisms of torque production in induction machines and dc machines

are similar, giving the ability to directly control the induction machine torque and achieve as quick torque response as in a dc machine.

Rapid developments in the field of power electronics, whereby better and more powerful semiconductor devices are available (with high switching speeds, high conducting currents, and very high blocking voltages that can be turned on and off, etc.), and where the power devices and circuits are packaged into a modular form. And the existence of powerful and inexpensive microprocessors which allow the complex control functions of the ac drive to be performed by utilizing software instead of expensive hardware, means that ac drives employing induction machines are more economical alternatives to adjustable speed dc drives. [1]

The development of high performance control schemes for ac drives driven by industry requirements, has followed a rapid evaluation during the past two decades. It is now recognized that the two highest performance control schemes of induction machine are field-oriented control (also called vector control VC), and direct torque control (DTC). They both aim to control effectively the machine torque and flux so as to force it to accurately track the command trajectory regardless of the machine and load parameter variations or any extraneous disturbance. Both control schemes have been successfully implemented in industrial products.

2.7.1 Vector Control of Induction Machine.

A central difference between a dc machine and an induction machine is that the torque and flux producing components of the induction machine stator current are not normally decoupled from each other, therefore, they cannot be controlled independently by applying direct methods.

With vector control, the objective is to control induction machines in the same manner described for dc machines, and thus obtain their excellent torque control and dynamic response, with simpler and more reliable machine.

Dc machines have stationary and orthogonal field and armature fluxes, vector controllers develop similar flux components in a rotating 2-axis co-ordinate system (model). These two components maintain orthogonality and are, therefore, independently controlled in all situations by control of their corresponding stator current components. To realize such a controller, a mathematical transformation is used to represent the three-phase stator current space vector $\boldsymbol{i}_s$ in an equivalent rotating 2-axis co-ordinate system. The three-phase stator current space vector $\boldsymbol{i}_s$ is stationary in space, with direction defined by stator windings along a-b-c axes shown in Figure (2.9) below. [18]

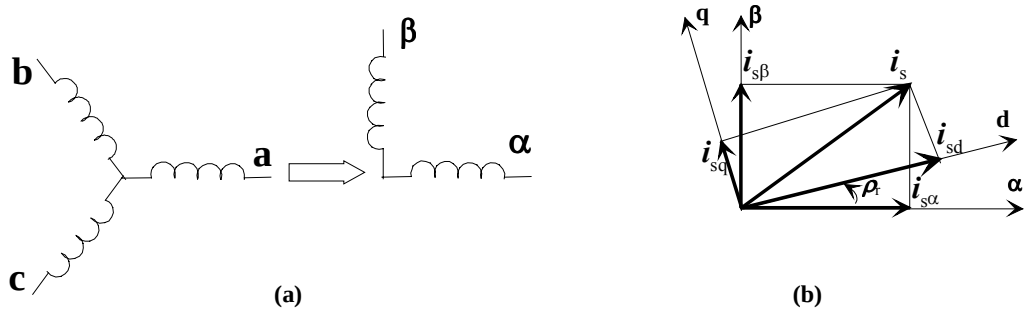

Figure 2.9. (a) 3 to 2 axis conversion. **(b)** Vector rotation. [18]

$$\boldsymbol{i}_s = \frac{2}{3}(i_a \,.\, e^{j0} + i_b \,.\, e^{j\frac{2\pi}{3}} + i_c \,.\, e^{j\frac{4\pi}{3}}) = i_{sd} + j \,.\, i_{sq} \qquad (2.15)$$

In rotating 2-axis form, the stator current space vector is resolved (decoupled) into a direct-axis (*d*-axis) flux-producing current component i_{sd}, and a quadrature-axis (*q*-axis) torque-producing current component i_{sq} [Equation (2.15)], with the *d*-axis fixed to the machine flux.

The instantaneous electromagnetic torque of the machine can then be expressed as the product of the flux-producing current and the torque-producing current, and since they are spaced 90° from each other, a maximum and fast torque response can be achieved using this model.

Figure (2.10) illustrates the block diagram of a conventional vector control scheme. A motor model is shown as a block in the figure, this model uses the concept of the 2-axis co-ordinate system described above (*d-q* axis) to model the motor equivalent circuit in the rotor-oriented reference frame. In the identification section, the rotor time constant τ is calculated, τ is an important parameter to keep the motor dynamic state balanced. [19]

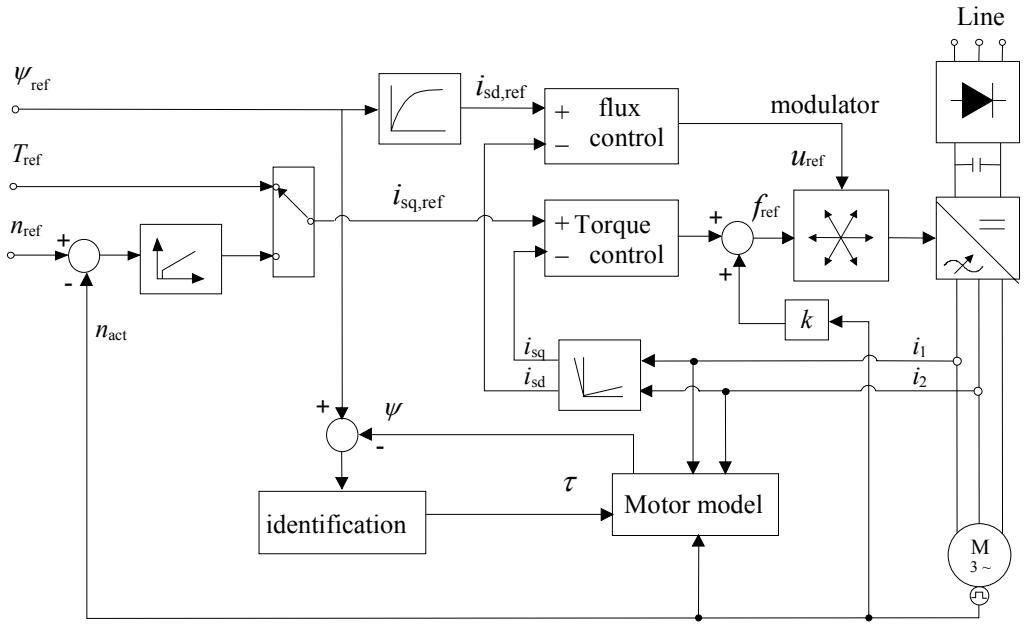

Figure 2.10. Block diagram of a conventional vector controlled induction motor drive [19].

Vector control of induction machines is a very effective control scheme that provides excellent control properties comparable to that of a dc machine. However, its implementation leads to a complex control system structure.

Another induction machine control scheme that has the same control properties of vector control but with significant reduction in the system complexity is the direct torque control (DTC) which is the subject of the next section.

2.7.2 Direct Torque Control of Induction Machine

Direct Torque Control (DTC) is an ac machine control scheme that embeds motor and inverter together and control them in a nearly optimal way. Since DTC is based on the theory of field-oriented control (discussed in the previous section), its objective is to achieve the necessary decoupling between the torque-producing component and the flux-producing component of the stator current space vector, leading to effective torque control with fast torque response.

In DTC the required decoupling is obtained by the use of on-off control, which can be related to the on-off operation of the inverter power switches. This implies that controllers based on DTC do not require a complex co-ordinate transformation, as was the case in vector control schemes. Consequently, a very simplified control structure and a high drive performance are achieved compared with drives utilizing vector control schemes. [14]

Concept of DTC

The basic idea of DTC is presented in Figure (2.11) below. The core of the system consists of three blocks: motor model, torque control, and optimum switching logic. The motor model estimates the actual torque, stator flux and shaft speed by means of measurements of two motor phase currents, the intermediate circuit dc voltage, and information on the state of the power switches. Torque and flux references are compared with the actual values and control signals are produced by using a two level hysteresis control method. Optimum switching is determined for every control cycle on a time level of 25 microseconds.

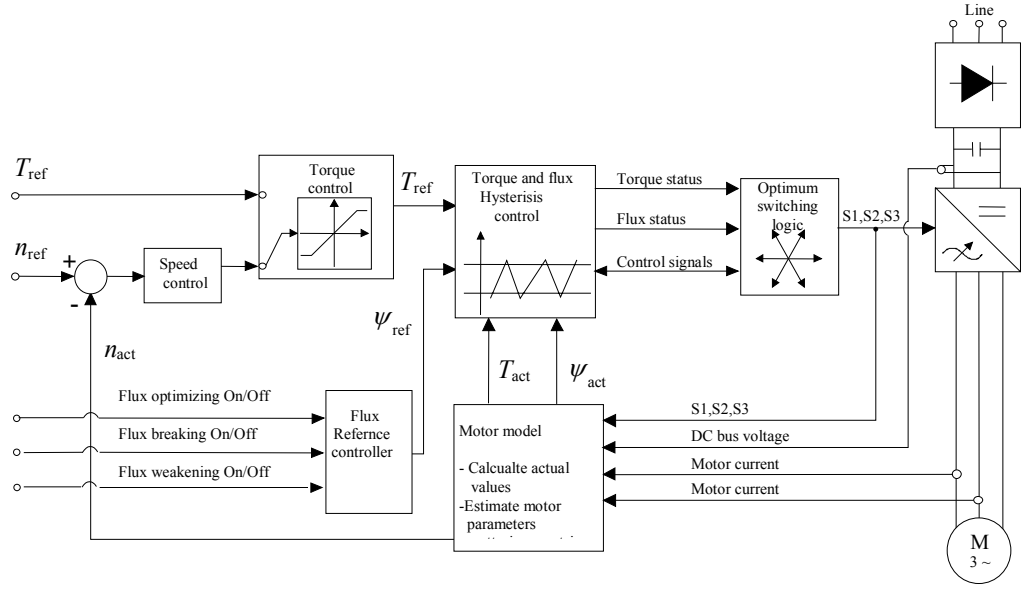

Figure 2.11. DTC controlled sensorless induction motor drive. [14]

Hysteresis Control of Stator Flux and Torque

Based on spatial vector representation, flux and current space vectors and inverter voltage space vectors can be represented e.g. in stator co-ordinate as in Figure (2.12) below.

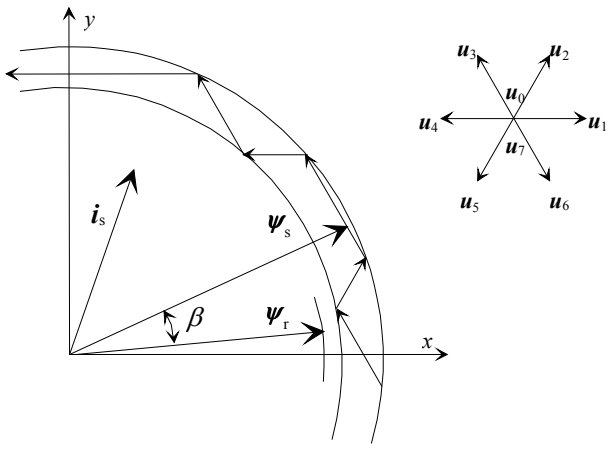

Figure 2.12. The stator flux space vector is controlled directly to achieve the required torque demand.

There are six voltage vectors and two different kinds of zero-voltage vectors available in the two level voltage source inverter. Torque is the cross product of stator current and flux or stator and rotor flux vectors [*see* Equation (2.14)]:

$$T_{\mathrm{e}} = \frac{3}{2} p \frac{1-\sigma}{\sigma L_{\mathrm{m}}} \boldsymbol{\psi}_{\mathrm{r}} \times \boldsymbol{\psi}_{\mathrm{s}} \tag{2.16}$$

The magnitude of the stator flux is normally kept constant and the motor torque is controlled by means of the angle β between the stator and the rotor flux. The rotor time constant τ of induction machine is typically longer than 100 ms, thus the rotor flux is stable and changes slowly compared with the stator flux. Consequently, it is possible to achieve the required torque very effectively by rotating the stator flux space vector directly in a certain direction as fast as possible.

In DTC, if more torque is needed, the purpose of the next power stage switching is to fulfil that demand. The instantaneous value of the stator flux vector is controlled in order to achieve the required motor torque. The stator flux vector is controlled by means of the inverter supply voltage.

The optimal switching logic defines the best voltage vector according to the actual value of torque and torque reference. The magnitude of the stator flux is also taken into account in the switch selection [14].

For example in Figure (2.12) the voltage vector $\boldsymbol{u}_4$ decreases effectively the radial component of the stator flux vector and, at the same time, it moves the flux vector tangential in the direction of rotation. The tangential movement causes the angle β and the torque to increase. The radial change affects the length of the stator flux, thus magnetization of the motor is also changed. The aim is to force the stator flux vector in the direction where both reference values of the torque and stator flux are achieved.

As the stator flux rotates, the effect of the voltage vector to the stator flux and torque changes. The switch references are altered only if the values of the actual torque and stator flux differ from their reference values by more than the allowed hysteresis. The behavior of hysteresis controlled torque is represented in Figure (2.13) below.

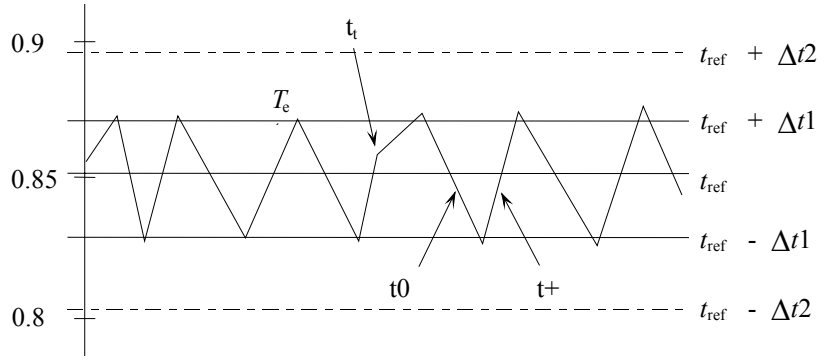

Figure 2.13. Hysteresis control of torque. [14]

Annotation t0 means that more torque is not needed and thus the zero voltage vector is selected. The actual value of the torque falls, so T_e decreases until the torque falls below the value $t_{ref} - \Delta t1$. After that, an appropriate voltage vector is selected in order to increase the torque (t+).

Motor Model

Accuracy of the motor model is very essential in DTC, because there is no feedback from the shaft speed [Figure (2.11)]. Only two stator phase currents are measured. The motor model is based on the identification of the motor parameters and current feedback.

The motor torque and speed are also estimated in the motor model. The main task of the motor model is to produce an accurate estimate of the stator flux linkage on every control cycle (25 microseconds). The stator flux linkage is calculated by means of the stator voltage vector and current:

$$\boldsymbol{\psi}_s = \int (\boldsymbol{u}_s - R_s \boldsymbol{i}_s)\, dt \tag{2.17}$$

The accuracy of the motor model is based on an identification run, which is made during commissioning. Main parameters of the motor model are motor inductances and stator resistance while the saturation effects of the inductances is also considered. [14]

2.8 Conclusion

The electric motors discussed throughout this chapter and the comparisons made between their dynamic performances and control schemes assists greatly in the process of selecting the right motor; and consequently, the right drive for the type of application considered in this work.

Induction motor drive incorporating squirrel-cage induction motor and employing direct torque control scheme is found to be the best alternative (among others) to suit such high demanding application, and therefore, it is selected to be an optimum solution for this electric drive application.

Induction motor drive of this type was found to have a simple, relatively cheap, and very effective torque and flux control with very fast torque response, satisfactory dynamic performance, and the lowest possible overall costs. These and many other well-known potentials of induction motor drives truly justify this selection.

3. PROTOTYPE DRIVE, DESIGN & RESULTS.

3.1 Introduction

In the previous chapter it was concluded that a squirrel-cage induction motor drive employing direct torque control scheme will have a satisfactory dynamic performance and a relatively low overall cost among other alternatives.

This combination promoted by the power of DTC provides a very precise knowledge and control of the drive load actual position over its whole duty cycle. Which is, in this case, absolutely essential for the proper operation and safety of the prototype drive.

This chapter will be devoted to the design and realization of a three-phase squirrel-cage DTC induction motor drive; the result should be a powerful, precise, and adequate motion control system which meets the beforehand set specifications.

3.2 Drive Specifications.

This prototype drive will be integrated in commercial physiotherapy and rehabilitation equipment. Typical applications of such equipment are:

- Analysis, assessment, and evaluation of musculoskeletal performance in rehabilitation clinics, sport centers, and research establishments.
- Detection and correction of muscular dysbalances which often lead to joint deterioration or irritation in movement patterns.
- A training machine used by different user groups, from early rehabilitation patients to strong athletes working sub-maximally or maximally.

There are several exercises (muscle actions) and training possibilities provided by such equipment, by carrying out a selected set of exercises (depending on the

type of treatment/training) the equipment can collect, process, and evaluate the user data to finally obtain an objective assessment of therapy or training. The drive to be designed here should, therefore, be able to fulfill all the conditions and requirements of such exercises. In fact, the whole prototype drive testing will be carried out based on these exercises, which consequently, necessitates a close look on these exercises and their physical meanings. This will be the subject of the next section.

3.2.1 Muscle Actions (Contractions)

The contraction of a muscle does not necessarily imply that the muscle shortens; it only means that tension has been developed by a muscle or a group of muscles. Muscles can contract in the following ways:

Isometric Contraction

This is a contraction in which no movement takes place, because the load on the muscle exceeds the tension generated by the contracting muscle. This occurs when a muscle attempts to push or pull an immovable object (e.g. pushing against the wall).

Isotonic Contraction

This is a contraction in which movement *does* take place, because the tension generated by the contracting muscle exceeds the moved load. This occurs, for instance, when you use your muscles to successfully push or pull an object. Isotonic contractions are further divided into two types: Concentric and Eccentric.

Concentric Contraction

This is a contraction in which the muscle decreases in length (shortens) against an opposing load. To help understanding this kind of muscle contraction, consider the case when the arm muscle or group of muscles are used to lift a load

weight up, as the weight moves up the muscles shortens. In this case, tension generated by the contracting muscle is opposite and exceeds the load weight.

Eccentric Contraction

This is a contraction in which the muscle increases in length (lengthens) as it resists a load. This occurs when a load weight is being lowered, so that tension generated by the contracting muscle is in the same direction and exceeds the load weight.

3.2.2 Load Mechanism

The load mechanism of this equipment is a kind of robotic arm, where the arm movement is limited to half a revolution (from 0 to 180°). The user (patient, athlete..) will apply a force on this arm and the function of the motor drive connected to the arm is to resist this force so as to keep the arm speed constant as well as to ensure that the arm will not be moved beyond its limits. Figure (3.1) below shows a basic non-detailed front view of the drive and arm (load) of this equipment.

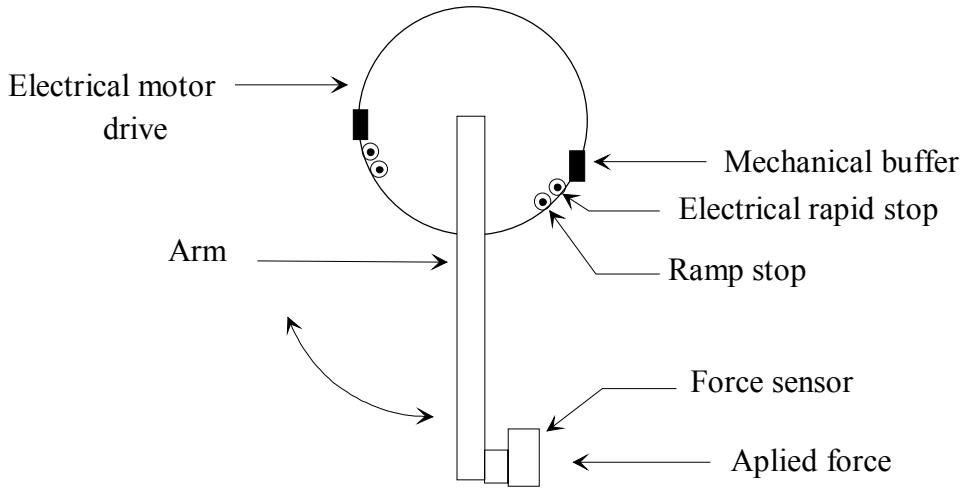

Figure 3.1. The load mechanism of the prototype drive. The distribution of safety electrical and mechanical switches on each side of the arm is shown. The force sensor passes a starting signal to the drive when a force is applied to it.

3.2.3 Electrical Specifications

The drive speed will follow a trapezoidal motion profile in its all modes of operation. Table (3.1) below gives the electrical requirements at the drive load.

Table 3.1. The electrical requirements (demands) at the load side of the prototype drive.

t_α	T_{Lmax}	ω_{max}	θ_{max}
100 ms	400 Nm	270 °/s	180°

Where :

t_α	Acceleration/deceleration time
T_{Lmax}	Maximum load torque the drive should be able to resist
ω_{max}	Maximum angular speed
θ_{max}	Maximum movable angle

3.2.4 Safety Requirements

The safety requirements of this equipment are very strict because of the direct interaction between the machine and humans; therefore, the load shaft should precisely follow its reference position command.

A DTC induction motor drive guarantees a safe behavior and a precise monitoring of the load shaft position. However, a machine of this type should be protected against abnormal operations and unexpected disturbances.

A set of safety switches should, therefore, be introduced to limit the drive load movement during abnormal conditions [*see* Figure (3.1)].

3.3 Selection of Technology

The general structure and components of a three-phase direct torque controlled squirrel-cage induction motor drive are shown in Figure (3.2). The system is integrated from five distinct elements: a power electronic frequency converter employing DTC, a squirrel-cage induction motor, a transmission system (gearbox) for speed reduction, a position encoder to keep track of the load actual position, and finally the load or the driven element.

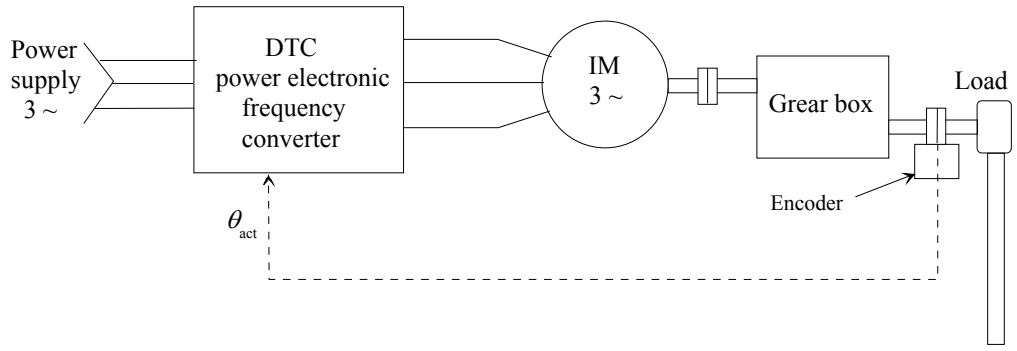

Figure 3.2. The general block diagram of a three-phase DTC induction motor drive (motion-control system). The figure shows the main components of the drive.

The above block diagram shows the main components of the electrical drive to be built in this project. The type, manufacture data sheet, and potentials of every component selected will be given next.

3.3.1 The Power Electronic Converter.

ABB has introduced in 1995 the first industrial, speed-sensorless DTC induction motor drive in the world. This contains the ACS 600 frequency converter (inverter), which uses power-plate IGBT modules.

The inverter switching directly controls the motor flux linkages and electromagnetic torque. The ACS 600 employs the concept of DTC, and can

accurately control the rotor speed and electromagnetic torque without encoder or tachometer feedback. [1]

The ACS 600 is a fully programmable frequency converter; a set of parameters can be optimized according to the motor, gear, encoder, and load to enable accurate and fast control of torque, speed and position of the drive. A list of the key parameters and their optimized values is given in Appendix (B).

Table (3.2) below gives information about the type and rating of the selected frequency converter.

Table 3.2. Technical data about the type and ratings of the selected three-phase power converter. [24]

Manufacturer	ABB
Type	Three-phase ACS 601-5-3
Nominal Power (P_n)	3 kW
Heavy duty Power (P_{hd})	2.2 kW
Nominal Voltage (U_n)	400 V
Nominal Current (I_n)	7.6 A

3.3.2 The Motor

This is a squirrel-cage, three-phase 4-poles induction motor. As was concluded in chapter 2, this motor provides the best compromise of satisfactory performance and low price compared to other alternatives.

In addition, this type of motor works in a perfect harmony with the above selected power converter to produce a high performance variable-speed electric motor drive. Table (3.3) below provides some technical data about the selected motor.

Table 3.3. Technical data of the selected three-phase induction motor. [15]

Manufacturer	ABB
Type	M2AA 90 L
Number of poles	4
Output Power (P_o)	1.5 kW (3 ~)
Nominal Torque (T_n)	10 Nm
Peak Torque (T_{max})	29 Nm
Nominal Speed (n_n)	1420 rpm
Nominal Voltage (U_n)	400 V
Nominal Current (I_n)	3.45 A
Frequency (f)	50 Hz
Moment of inertia (J)	0.0043 kgm^2
Power factor (cos φ)	0.79
Efficiency (η)	80.3 %

3.3.3 The Gearbox

A gearbox is required to match the motor to the load, since the motor must provide peak torques at specified speeds. The gearbox both reduces the motor speed and steps up the motor torque to achieve a proper matching between the motor output and the load demand.

The efficiency of the gearbox in a motion control system is an important factor for the accuracy of the system as a whole. Planetary gearboxes are characterized by their high efficiency, minimized backlash (lost motion inside the gearbox), compact design, and high gear ratio to gear size.

For these excellent properties of planetary gearboxes, a gearbox of this type with the proper gear ratio were selected and integrated in the prototype drive. The technical data of the selected gearbox is given in Table (3.4) below.

Table 3.4. Technical data of the selected gearbox. [25]

Manufacturer	TRANSMITAL BONFIGLIOLI
Type	Planetary 300L2 series.
Gear ratio (n)	20.1
Gear moment of inertia (J)	0.000314 kgm^2 (referred to the motor side)
Input speed	2000 rpm
Efficiency	0.94
Nominal torque	700 Nm
Maximum torque	840 Nm

3.3.4 The Position Encoder

In any motion control system, information about the actual position of the load shaft at every instance of a positioning cycle is very essential for the proper control and safety of the system.

A high-resolution absolute position encoder is, therefore, mounted on the load shaft of the drive. Its function is to measure and feedback the load shaft actual position to the converter, which will then compare the actual position value with the set position reference value and use the result to force the drive to follow its command trajectory.

It is also important to know that the resolution of the absolute encoder plays a vital role in the accuracy and safety of the system. Table (3.5) gives the technical data of the selected absolute encoder.

Table 3.5. Technical data of the selected absolute position encoder. [26]

Manufacturer	Stegmann
Type	AG 615, gray code.
Resolution	8192 steps/revolution
Message length	13 bits

3.4 Drive Simulation Model

In this kind of drive systems, the motor drives the load through some kind of transmission system (gearbox). The fundamental relationship that describes such system is:

$$T_{\mathrm{m}} = T_{\mathrm{s}} + J_{\mathrm{tot}} \frac{\mathrm{d}\,\omega_{\mathrm{m}}}{\mathrm{d}\,t} + \xi\omega_{\mathrm{m}} \tag{3.1}$$

Where:

J_{tot}	the system total polar moment of inertia, that is, the inertia of the gearbox and load referred to the motor shaft, plus the inertia of the motor's rotor in kgm^2, for simplicity it will be denoted as J.
ξ	the damping constant in $\mathrm{Nm\ rad^{-1}s}$
ω_{m}	the angular velocity of the motor shaft in $\mathrm{rad\ s^{-1}}$
T_{s}	the torque required to drive the load referred to the motor shaft in Nm, it includes the external load torque and other friction loads
T_{m}	the torque developed by the motor

When the torque required to drive the load (that is $T_{\mathrm{s}} + \xi\omega_{\mathrm{m}}$) is equal to the supplied torque, the system is in balance and the speed will be constant. The load accelerates or decelerates depending on weather the supplied torque is greater or lower than the required driving torque. Therefore, during acceleration, the motor has to supply not only the output torque but also the torque which is required to accelerate the inertia of the rotating system. [27]

The purpose of the drive simulation model is to find out if the above selected components will perform according to the drive specifications, and to see if the resultant drive can reach the required maximum values defined in Table (3.1).

The simulation model will be built according to Equation (3.1) above, a suitable representation of the instantaneous angular velocity in terms of system torques and inertia can be found by the application of Laplace Transform to Equation (3.1) and solving for $\omega_{\mathrm{m}}(\mathrm{s})$:

$$\omega_{\mathrm{m}}(\mathrm{s}) = \frac{T_{\mathrm{m}} - T_{\mathrm{s}}}{(J\,\mathrm{s} + \xi)} \tag{3.2}$$

The above equation can be represented by the following block diagram

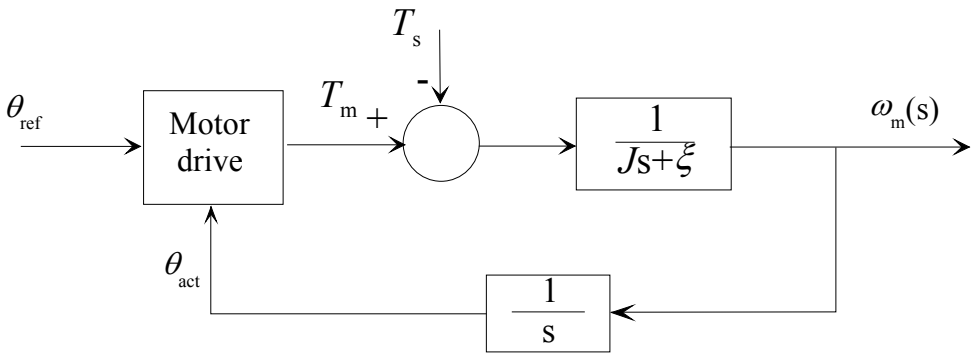

Figure 3.3. Block diagram representation of Equation (3.2). The prototype drive is simulated based on this block diagram.

The drive performance can then be simulated based on this block diagram. One of the important requirements that were set in the drive specifications [section (3.2)] is the drive acceleration/deceleration time t_{α} in Table (3.1). It was specified that the drive should be able to accelerate/decelerate in no more than 100 ms. It is, therefore, necessary to simulate the selected drive and find out beforehand if it will be able to achieve this requirement.

The simulation will be performed assuming a worst case condition where the load torque (T_{s}) is a maximum [i.e. when $T_{\mathrm{s}} = \frac{T_{\mathrm{Lmax}}}{n}$ in Table (3.1)]. The damping constant (ξ) was found to be 0.004 Nm rad^{-1} s [*see* Appendix (A)], other

friction torques (caused e.g. by bearings or other system inefficiencies) are assumed to be small, and therefore, are not considered in this simulation.

The motor torque T_m in Figure (3.3) will be assumed to have a very fast rise time in response to a step rise of load torque, and therefore, the simulation model can be simplified through representing the motor torque by a step function (step torque). To justify this assumption, Figure (3.4) below, shows experimental results obtained with the speed sensorless ABB DTC induction motor drive using a voltage-source inverter (ACS 600) [14]. The figure shows the measured temporal variation of the electromagnetic torque for a 70% torque reference step at 25 Hz. The resultant torque response (torque rise) seen from the figure is very fast (rise time less than 2 ms).

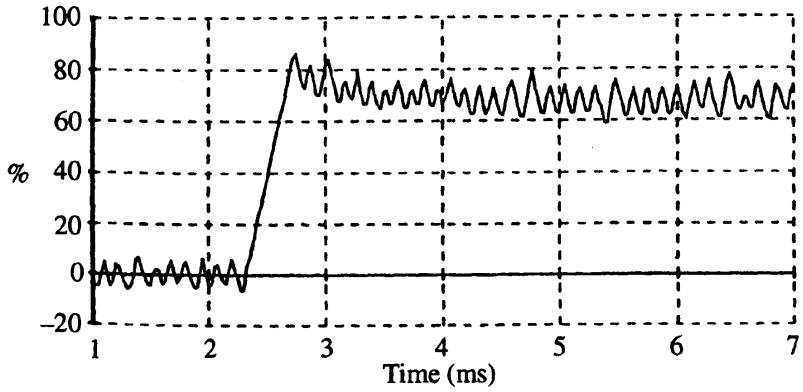

Figure 3.4. The estimated air-gap torque for a 70 % torque reference step at 25 Hz. [14]

However, a rise time as short as this will not be used in this simulation since at nominal speed where the voltage reserved is low, the torque response is probably somewhat slower. As a worst case study, the rise time of the motor torque will be set to 10 ms in this simulation.

The simulation model [shown in Appendix (A)] is built and executed using the program SIMULINK, the resultant speed versus time curve is shown in Figure (3.5) below. The figure shows clearly that the drive will be able to accelerate to its set maximum speed (270 °/s) in about 15 ms.

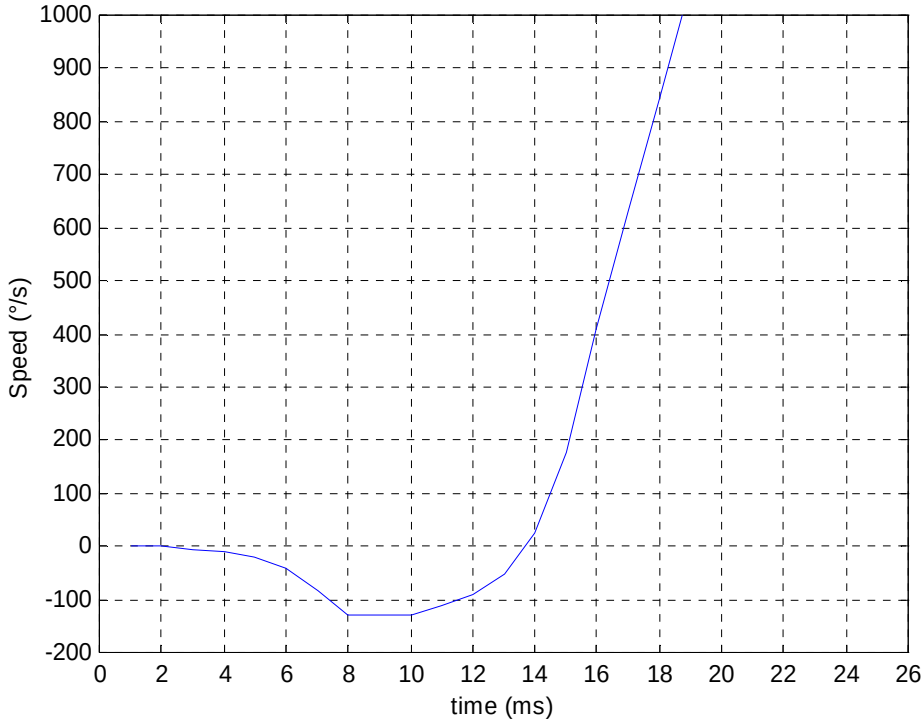

Figure 3.5. Simulation results for the drive angular velocity versus time. The acceleration time corresponding to 270 °/s is about 15 ms.

Despite the fact that some assumptions and approximations were made to accomplish this simulation, the above result is still considered valid as it initially proves that the drive will function according to its set specifications under worst case condition. The negative speed that appears in Figure (3.5) is due to a maximum load torque (T_s) instantly (zero rise time) applied to the drive shaft, while the motor torque is lagging behind with a slower rise time of 10 ms.

3.5 Drive Duty Cycle

In this phase of the project, adequate knowledge of the drive final (real) duty cycle is not available; hence, calculations of its worst case duty cycle will be given here. One of the aims in this context is to find out the worst case duty cycle time intervals and to ensure that even when the drive runs at its worst case load speed and torque, it is still able to move the specified distance without violating the motor thermal conditions.

One successful approach to the duty cycle calculations is to find out the effective torque spent by the motor during each successive duty cycle and compare it with the motor nominal torque. As long as the mentioned effective torque is less than or at most equal to the motor nominal torque, the motor thermal status is considered stable. The effective motor torque can be calculated based on Equation (3.1) above. A general (trapezoidal) motor motion profile and its corresponding motor torque profile are given in Figure (3.6), (a) and (b) respectively.

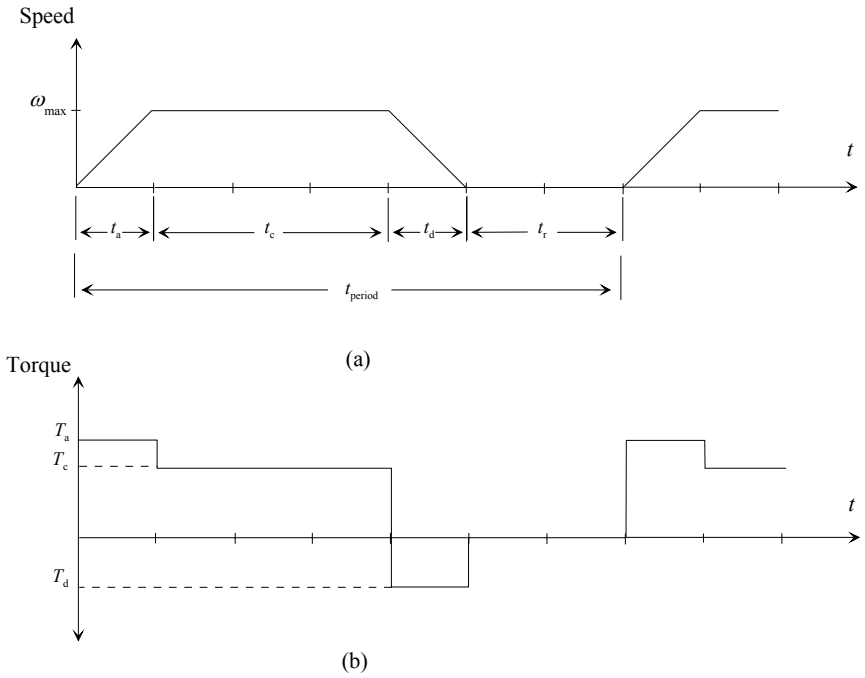

Figure 3.6. The motor trapezoidal motion profile and its corresponding torque profile for the case considered.

Within the given cycle (t_{period}), four time intervals exist: t_a, t_c, t_d, and t_r with their corresponding motor torques T_a, T_c, T_d, and T_r. Where t_a is the acceleration time interval, t_c is the constant speed time interval, t_d is the deceleration time interval, and t_r is the drive rest time interval. From Figure (3.6 b), the value of the effective torque can be found as:

$$T_{\text{eff}} = \sqrt{\frac{T_{\text{a}}{}^2 t_{\text{a}} + T_{\text{c}}{}^2 t_{\text{c}} + T_{\text{d}}{}^2 t_{\text{d}} + T_{\text{r}}{}^2 t_{\text{r}}}{t_{\text{period}}}} \tag{3.3}$$

The constant speed time t_c can be calculated by rearranging Equation (3.3) and taking $T_{\text{eff}} = T_n = 10$ Nm with $t_{\text{period}} = t_a + t_c + t_d + t_r$, the result is:

$$t_{\text{c}} = \frac{T_{\text{eff}}{}^2 (t_{\text{a}} + t_{\text{d}} + t_{\text{r}}) - (T_{\text{a}}{}^2 t_{\text{a}} + T_{\text{d}}{}^2 t_{\text{d}})}{(T_{\text{c}}{}^2 - T_{\text{eff}}{}^2)} \tag{3.4}$$

From Table (3.1) the load maximum torque referred to the motor side is $T_{\text{MLmax}} = \frac{T_{\text{Lmax}}}{n} = \frac{400}{20.1} = 19.9\text{Nm}$, the load maximum angular speed referred to the motor side is $\omega_{\text{Mmax}} = \omega_{\text{max}} . n = 270 \times 20.1 = 5427 \frac{\text{Degrees}}{\text{s}} = 94.72 \frac{\text{rad}}{\text{s}}$, the required motor maximum acceleration is $\alpha_{\text{Mmax}} = \frac{\omega_{\text{Mmax}}}{t_\alpha} = \frac{94.72}{0.1} = 947.2 \frac{\text{rad}}{\text{s}^2}$, and $t_a = t_d = t_\alpha = 0.1$ s.

From Equation (3.1), the motor acceleration torque T_a is given by:

$$T_{\text{a}} = T_{\text{MLmax}} + J\alpha_{\text{Mmax}} + \xi\omega_{\text{Mmax}} = 24.65 \text{ Nm} \tag{3.5}$$

While the motor deceleration torque T_d is given by:

$$T_{\text{d}} = T_{\text{MLmax}} - J\alpha_{\text{Mmax}} + \xi\omega_{\text{Mmax}} = 15.9 \text{ Nm} \tag{3.6}$$

And the motor torque in the constant speed time interval T_c is given by:

$$T_{\text{c}} = T_{\text{MLmax}} + \xi\omega_{\text{Mmax}} = 20.28 \text{ Nm} \tag{3.7}$$

Since adequate knowledge about the drive real duty cycle and the different time intervals involved is not available, the duty cycle is calculated here for a range of speeds from 30 to 270 °/s. For every speed the values of the different time intervals are calculated. The maximum position moved (θ_{max}) during one cycle $t_{period} = t_a + t_c + t_d + t_r$ (assuming a trapezoidal motion profile) can be expressed as:

$$\theta_{max} = \frac{1}{2}\omega_L t_a + \omega_L t_c + \frac{1}{2}\omega_L t_d \tag{3.8}$$

Where ω_L is the Load speed (speed range). From Equation (3.8) and based on the fact that the load movement in this case is limited to an angle of 180° (the maximum angle moved within any duty cycle will not exceed 180°), it is possible to calculate the constant speed time interval t_c as:

$$t_c = \frac{\theta_{max}}{\omega_L} - \frac{1}{2}(t_a + t_d) \tag{3.9}$$

After finding the value of t_c for a range of motor speeds, it is now possible to calculate the minimum rest time interval t_r during which the motor should be allowed to rest between every repetitive working cycle. From Equation (3.3) with $t_{period} = t_a + t_c + t_d + t_r$, the result is:

$$t_r = \frac{(T_a^{\,2} t_a + T_c^{\,2} t_c + T_d^{\,2} t_d) - T_{eff}^{\,2}(t_a + t_c + t_d)}{T_{eff}^{\,2}} \tag{3.10}$$

the calculated values of t_c and t_r for a range of motor speeds are given in Table (3.6) below.

Table 3.6. Calculation of the duty cycle time intervals for a range of motor speeds. The moved angle is 180° and the load torque is 400 Nm.

ω_L (°/s)	t_c (seconds)	t_r (seconds)	t_{period} (seconds)
30	5.9	95	101.1
60	2.9	48.45	51.55
90	1.9	33	35.1
120	1.4	25	26.6
150	1.1	20.5	21.8
180	0.9	17.5	18.6
210	0.76	15	15.96
240	0.65	13.5	14.35
270	0.57	12.1	12.87

Note that the rest time t_r is 5 times longer than the value found from Equation (3.10). This had to be done because during the rest time t_r the motor and its cooling fan are not running (motor is air-cooled using a fan connected to its rotor). Hence, the effective cooling of the standing motor is only about 20% of its value when the motor is running at its nominal speed. [28]

From the table above, it is notable that at low speeds (e.g. 30 °/s) the positioning cycle (t_{period}) is very long (101.1 s), the rest time compose the major part of it. The reason for this is that the load torque as well as the acceleration/deceleration torques are higher than the motor nominal torque, therefore, the motor should be allowed to rest for long periods of time if it has to operate at low speeds with maximum torque. It is perhaps possible to operate the drive at low speeds for shorter times than the values calculated here, however, in that case the motor thermal time constant should be taken into consideration.

Another worst case scenario to be considered here is a one that follows a triangular motion profile. In this case $t_c = 0$, and it is required to calculate the minimum drive rest time t_r. From Equation (3.3) above, t_r is found to be:

$$t_r = 5 \times \frac{(T_a^2 t_a + T_d^2 t_d) - T_{eff}^2 (t_a + t_d)}{T_{eff}^2} = 3.3\text{s} \qquad (3.11)$$

And t_{period} = 3.5 s in this case. So if for any reason the drive has to operate in this kind of situation, it should be allowed to rest for at least 3.3 s before starting the next accelerate/decelerate cycle.

3.6 Description of the Tests

The objective of these tests is to verify (practically) that the prototype drive will perform according to the specifications and requirements given in Table (3.1). One way to do this is to measure the drive maximum values and compare it to the values in that table.

However, a more precise and confident performance test can be made in accordance with the final product (physiotherapy equipment) real functions, which means that tests based on the various exercises (muscle actions) introduced in section (3.2.1) should be considered.

3.6.1 The Test Bench

In a real world usage, a human will carry out these exercises as part of his/her treatment/training program at the load side of the drive. Therefore, it may seem to be advantageous to make the drive tests on humans. However, for many reasons especially safety, the tests were made via a relatively large dc machine connected to the load shaft of the prototype drive.

The dc machine in this case, will act as the load of the drive, it will resemble human actions in different exercises; this will be explained in accordance with every test made. An illustrative sketch of the resultant test bench is shown in Figure (3.7) below, while a snapshot of the real test bench is given in Appendix (E).

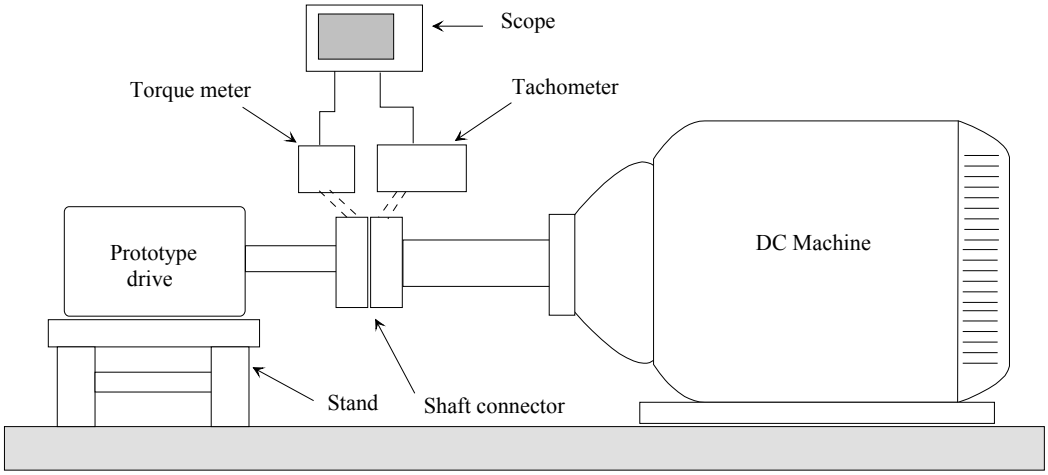

Figure 3.7. A side view of the prototype drive test bench. The dc machine resembles human actions in different exercises. The load speed and torque are measured directly from the shaft.

The ratings of the dc machine shown in Figure (3.7) are given in Table (3.7) below. The tachometer and torque meter shown in the figure reads the shaft actual speed and torque, respectively. The read signals are fed into the oscilloscope where it is possible to view and save the test results. In all the tests made, the dc machine is speed controlled while the prototype drive is speed-position controlled.

Table 3.7. Ratings of the dc machine.

Manufacturer	Strömberg Oy
Nominal Power (P_n)	180 kW
Nominal Torque (T_n)	1146 Nm
Nominal Speed (n_n)	1500 rpm
Nominal Voltage (U_n)	440 V
Nominal Current (I_n)	435 A

3.6.2 The Test Results

Here the prototype drive will undergo various tests; the ability and adequacy of the drive to suit and manage the above mentioned exercises with the required position accuracy and acceleration/deceleration times, forms the major part of the

testing process, and therefore, will be given first. Test results for the electrical safety switches and the drive response time to their prompts are given next.

Isometric Exercise

In pushing against an immovable object, the human muscles generate less tension than required to move the object. To realize such a test with the above described test bench, the dc machine output torque is limited to a value less than that of the prototype drive. While setting the positioning speed of the later to zero (since speed-position control is used in the prototype drive, when the positioning speed is set to zero the motor will not rotate –unless rotated by an external irresistible torque- regardless of the values of the reference and target positions).

When both machines are run, the dc machine will exert a force that attempts to rotate the shaft and the prototype drive will resist that movement and try to keep a zero shaft speed (in accordance with its positioning speed). The results of this test for a range of load torques (dc machine output torques) are given in Table (3.8) below.

Table 3.8. Test results for the isometric exercise. A load torque up to 602 Nm was recorded. T is the inverter torque limit as a percentage of T_n.

Test	Prototype drive		Load shaft	
No.	ω (°/s)	T (%T_n)	ω (°/s)	T (Nm)
1	0	100	0	70
2	0	100	0	157
3	0	100	0	233
4	0	100	0	314
5	0	100	0	390
6	0	100	0	465
7	0	100	0	579
8	0	100	0	580
9	0	100	0	602

A draw of the signals stored for test number 9 is given in Figure (3.8). The figure indicates that the prototype drive was able to successfully resist a load torque of more than 600 Nm for a time period of 10 seconds without collapsing

(the speed of the shaft remains zero during all the tests). Comparing this value (600 Nm) to the maximum load torque (T_{Lmax}) in Table (3.1) verifies the drive torque adequacy.

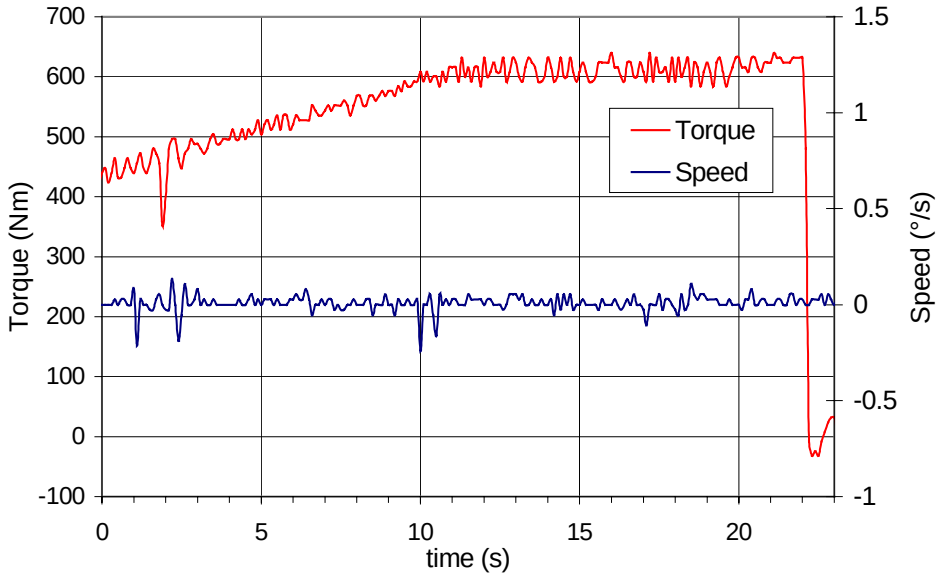

Figure 3.8. Torque and speed curves for isometric exercise, test number 9. The figure shows that the prototype drive was able to resist 600 Nm for 10 seconds (shaft speed = 0).

Isotonic Exercise

The situation here is similar to pushing against a *movable* object, this exercise with its two forms; Concentric and Eccentric is used specially for muscle training. In this case the prototype drive output torque is limited to a value lower than that of the dc machine and the drive positioning speed is set to zero. The dc machine reference speed is higher than zero, hence, the dc machine will exert a force (load torque) that attempts to rotate the shaft and the prototype drive will try to resist the movement by putting forth its maximum available torque. The prototype drive will work in this case as a generator.

Since the dc machine is given a higher torque capability, when its exerted torque becomes higher than the prototype drive torque limit, the shaft will start rotating slowly to the target position. The results of this test for different torque limits are

given in Table (3.9) below, note the effect of the inverter current limit I on the test results. In test number 6, for example, when $I = I_n$ and with a torque limit of 70 % the nominal, the prototype drive output torque was only 100 Nm. However, in test 11 with $I = 1.5\ I_n$ it was 300 Nm even though the drive torque limit was only 45 % the nominal.

Table 3.9. Results of the isotonic exercise. A load torque of 300 Nm was recorded. T is the inverter torque limit as a percentage of T_n. I is the inverter current limit as a percentage of I_n

Test	Prototype drive		dc machine	Load shaft	
No.	I (%I_n)	T (%T_n)	T (%T_n)	Status	T (Nm)
1	100	0	10	OK*	70
2	100	5	10	OK	70
3	100	10	15	OK	70
4	100	20	15	OK	140
5	100	50	25	OK	70-80
6	100	70	15	OK	100
7	100	80	15	OK	110
8	80	70	15	OK	220
9	80	84	20	OK	300
10	150	43	19	OK	290
11	150	45	20	OK	300

* The shaft moves slowly without any faults.

A plot of test number 11 is given in Figure (3.9) below.

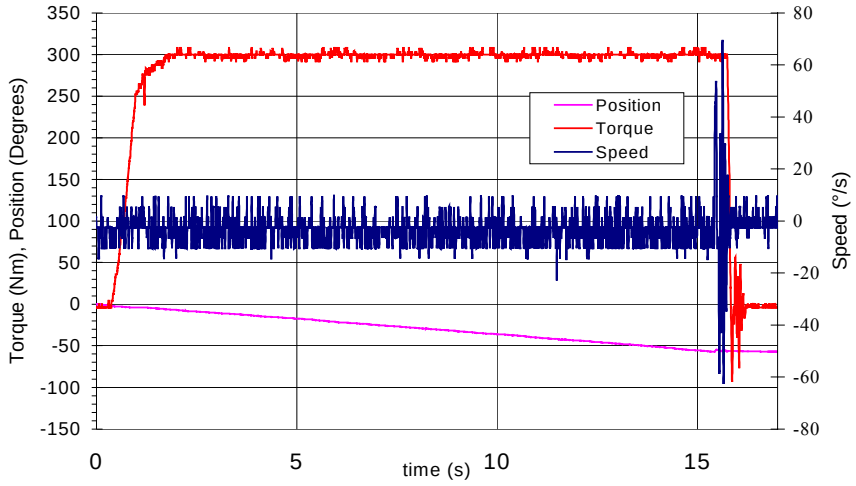

Figure 3.9. Torque, speed, and position curves for isotonic exercise, test number 11. After the load torque exceeds the prototype drive torque limit, the shaft starts moving slowly (about 5 °/s) to the target position.

The average value of the shaft speed is very small (4 - 5 °/s), however, it is clear from the figure (position curve) that the shaft has moved from 0 to about 55° with a recorded shaft (load) torque of 300 Nm. During the isotonic tests the prototype drive has shown a desirable behavior without undergoing any faults.

Positioning Tests

These are tests made to measure the position accuracy of the prototype drive under different values of load torque and shaft speed. The prototype drive is given a position reference and a higher torque limit than the dc machine, so that the prototype drive will dominate the dc machine and move the load shaft on its own speed and to its target position (the prototype drive is in a motoring mode). In the final product, this type of test can be performed to measure the user-exerted force (torque) on the drive load.

Two kind of tests were made here; the first with both dc machine and prototype drive rotating in the same direction, and the second with the machines rotating in opposite directions. This corresponds to the user being pressing or resisting the drive lever arm, the test results for the first case are given in Table (3.10) below.

Table 3.10. Results of the positioning test with dc machine and prototype drive rotates in the same direction. The starting position is 0° and the target (reference) is 180°. T is the inverter torque limit as a percentage of T_n.

Test	Prototype drive		dc machine	Load shaft	
No.	ω (°/s)	T (%T_n)	T (%T_n)	Status	T (Nm)
1	60	100	40	OK*	250
2	90	100	20	OK	300
3	90	100	15	OK	200
4	180	100	6.3	OK	90
5	250	100	7.4	OK	100

* The shaft moves without any faults.

Test number 5 is plotted in Figure (3.10) below, the load torque is around 100 Nm and the load speed is equal to the prototype drive positioning speed (250 °/s).

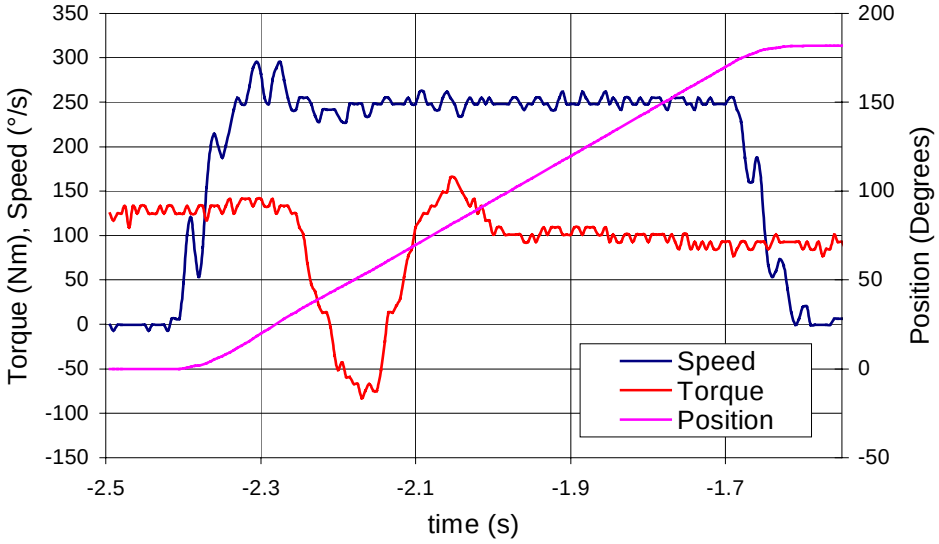

Figure 3.10. Torque, speed, and position curves for positioning test, test number 5 with dc machine and prototype drive rotating in the same direction. The starting position is 0° and the target (reference) is 180°.

The torque curve shown in Figure (3.10) drops to a negative value at the moment after the drive finishes accelerating the load; this behavior is perhaps due to the drive speed controller being not sufficiently optimized.

Next, tests were made with the dc machine rotating in opposite direction to that of the prototype drive, the results are given in Table (3.11) below. In every test made, the prototype drive has successfully moved from its starting position (0°) to its target position (-180°), while forcing the load (dc machine) to move according to its set positioning speed and direction of movement.

For example in test number 2, at low speed (30 °/s) and high load torque (300 Nm) the test was successful. Again in test 15, at high speed (390 °/s) and high load torque (300 Nm) the prototype drive is still dominating the load (dc machine) and forcing it to behave in the desired manner.

Table 3.11. Results of the positioning test with dc machine and prototype drive rotating in opposite directions. The starting position is 0° and the target (reference) is -180°. T is the inverter torque limit as a percentage of T_n.

Test	Prototype drive		dc machine	Load shaft	
No.	ω (°/s)	T (%T_n)	T (%T_n)	Status	T (Nm)
1	30	100	10	OK*	160
2	30	100	20	OK	300
3	60	100	10	OK	160
4	60	100	20	OK	300
5	60	100	20.3	OK	320
6	90	100	10	OK	160
7	90	100	20	OK	300
8	120	100	10	OK	160
9	120	100	20	OK	300
10	180	100	10	OK	160
11	180	100	20	OK	300
12	270	100	10	OK	160
13	270	100	20	OK	300
14	390	100	10	OK	160
15	390	100	20	OK	300

* The shaft moves without any faults.

An illustrative plot of test number 15 is shown in Figure (3.11) below.

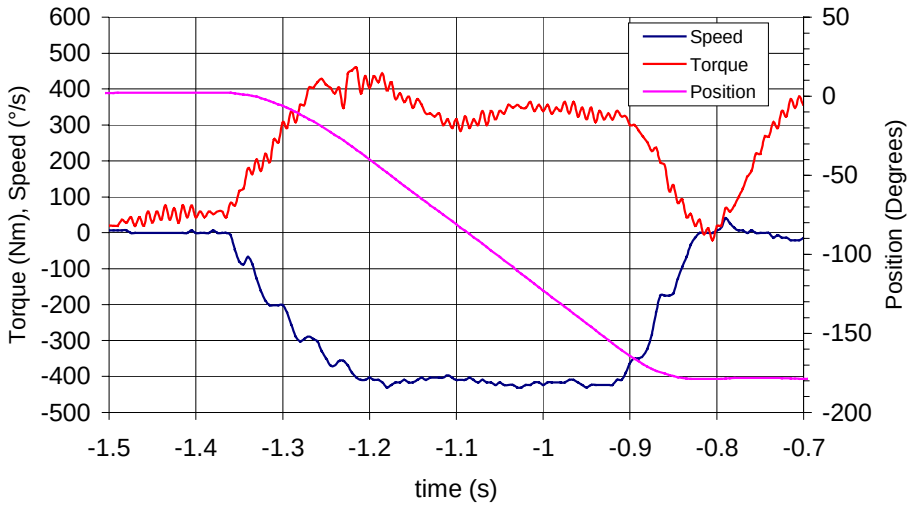

Figure 3.11. Torque, speed, and position curves for the positioning test, test number 15 with dc machine and prototype drive rotating in opposite directions. The starting position is 0° and the target (reference) is -180°.

The position curve shown in the figures above is pretty smooth, even though the load speed and torque are around their maximum values. This is a very desired property in applications like the one considered here. It also means that the drive is taking full control on its load over the whole positioning interval.

During all the positioning tests, the prototype drive position accuracy was very high. A position error of less than 0.1° was recorded between the drive set position reference and the actual position reached.

In Table (3.1), the acceleration/deceleration time t_α is required to be less than 100 milliseconds (ms). To practically confirm the ability of the prototype drive to accelerate/decelerate within this time, some no load tests at speed range from 60 to 360 °/s were made.

In this case, the only load torque on the drive is that due to the shaft connector and rotor inertia of the dc machine. The no load tests result are given in Table (3.12) below. Note that in every one of the four tests made, the value of t_α is below 100 ms, and values as small as 40 ms (in test number 1) were achieved, this comes in a good agreement with the results achieved in the prototype drive simulation introduced in section (3.4) above.

Table 3.12. Results of the no load test. The starting position is 0° and the target (reference) is 180°. T is the inverter torque limit as a percentage of T_n.

Test	Prototype drive		Acc./Dec. time	dc machine	Load shaft	
No.	ω (°/s)	T (%T_n)	t_α	T (%T_n)	Status	T (Nm)
1	60	100	~ 40 ms	0	OK*	14
2	120	100	~ 70 ms	0	OK	14
3	180	100	~ 60 ms	0	OK	14
4	360	100	~ 80 ms	0	OK	14

* The shaft moves without any faults.

Safety Switches

During any positioning cycle, the failure of the drive to stop on the desired target position due to an external disturbance or abnormal operation may cause serious injury to the human working on the drive load.

To assure that the drive load will not be moved beyond its desired limits or safe operating area (even during abnormal conditions), a set of electrical and mechanical position limits are introduced. These limits were shown in Figure (3.1) above.

The electrical limits (inductive switches) are classified into two types; the function of the first is to reduce the speed of the arm, this type is called ramp stop. The function of the second is to rapidly stop the arm as it passes over it, this type is therefore called the rapid stop.

Four electrical limits are used in the prototype drive, two on each side of the arm. On one side, the ramp stop is placed in front of the rapid stop with respect to the arm, so that when the arm (for any reason) moves beyond its operating region, it first passes the ramp stop. The ramp stop will act to reduce the speed of the arm before it reaches the rapid stop that will stop it almost instantly.

The mechanical buffers (limits) are used for emergency purposes in case the electrical switches fail to stop the arm. They should be capable to stop the arm instantly without any damage even at maximum speed and torque.

The response time, which is the time taken by the drive to stop the arm after receiving a control signal from the switch, is measured in these safety tests. The test results for the rapid stop safety limit are given in Table (3.13). The response time is 40 ms regardless of the arm speed and load torque.

Table 3.13. Test results of the drive response time to a trigger signal from the rapid stop safety limit. The response time is 40 ms. T is the inverter torque limit as a percentage of T_n.

Test	Prototype drive		Load torque		Rapid stop
No.	ω (°/s)	T (%T_n)	T_L(Nm)	Status	Response time (ms)
1	30	80	70	OK*	~ 40
2	30	80	315	OK	~ 40
3	60	100	0 (no load)	OK	~ 40
4	120	100	315	OK	~ 40
5	240	80	0	OK	~ 40
6	240	80	70	OK	~ 40
7	240	80	315	OK	~ 40
8	240	80	465	OK	~ 40
9	240	100	580	OK	~ 40

* The arm stopped without faults

Figure (3.12) below shows a plot of test number 5, the response time read from the figure is even less than 40 ms.

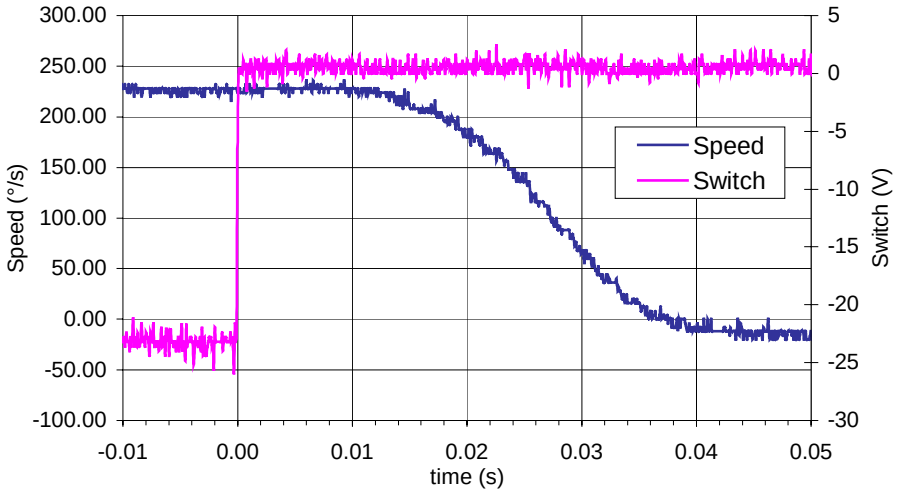

Figure 3.12. Speed curve versus rapid stop triggering signal recorded while testing safety switches, test number 5 above. The response time read from this figure is less than 40 ms.

It is possible to roughly calculate the angle (stop delay) that the arm will move from the point when it passes the switch to the point when the drive stops it . In

Figure (3.12) and from the point the switch triggers, t_c = 0.01 s, t_d = 0.03 s and from Equation (3.8) above:

$$\theta_{\text{delay}} = 240 \times 0.01 + \frac{240}{2} \times 0.03 = 6° \tag{3.12}$$

3.7 Conclusion

In this chapter, a description of the design and performance test results of a DTC squirrel-cage induction motor drive was given. Testing of the prototype drive has shown that the drive will have a satisfactory performance and high position accuracy. The ability of the drive to successfully operate at high values of load torque and speed comparable to those given in Table (3.1) was also demonstrated in the tests.

Also calculations of the drive worst case duty cycles and their related values (limits) were introduced before testing the drive. The achieved results with the most significant values recorded during the tests are summarized in Table (3.14) below. These values can be compared to the values given in Table (3.1) to see to what degree the drive can follow its set specifications.

Table 3.14. A summary of the significant values recorded during the prototype drive tests.

Maximum load torque at zero speed	600 Nm
Load torque during drive run (T_{Lmax})	400 Nm
Maximum driving speed achieved (ω_{max})	400 °/s
acceleration/deceleration time (t_{α})	40 ms
Response time to safety limit	40 ms
Stop delay θ_{delay}	6°
Position error	Less than 0.1°

4. CONCLUSIONS

The ultimate result of this thesis is the design and realization of a three-phase variable-speed direct torque controlled squirrel-cage induction motor drive that meets beforehand set specifications of high performance and relatively low price.

In chapter two, a detailed study of different motors and drive solutions available in the market today was given. Induction motor drive incorporating squirrel-cage induction motor and employing direct torque control scheme was found to have a simple, relatively cheap, and very effective torque and flux control with fast torque response, satisfactory dynamic performance, and the lowest possible overall costs. Hence, it was adopted here for this application.

In chapter three, a complete description of the design and performance test of the selected drive was given. The drive simulation and results as well as calculations of the drive worst case duty cycles and their related values were also given. The selected drive was proven to behave according to the beforehand set specifications through a set of performance tests. A safety plan was also introduced and tested in this chapter.

Perhaps the only drawback of this drive is its relatively large size. A drive with smaller size and comparable performance can be achieved by utilizing, for example, brushless dc motor drive or disc armature dc motor drive (*refer* to chapter two for more details). However, such a drive will be with no doubt much more expensive than induction motor drive of the type described above.

REFERENCES

[1] Peter Vas, “Sensorless Vector and Direct Torque Control”, Oxford University Press, 1998.

[2] D. W. Novotny and T. A. Lipo, “Vector Control and Dynamics of AC Drives”, Clarendon Press Oxford 1997.

[3] PARVEX Servo Systems, DC Servomotors TF Series, PVD 3372 07.89.

[4] PARVEX Servo Systems, Disc Armature DC Servomotors, AXEM, Series F, MC and MD, PVD 3345 – 06/89.

[5] T. Kenjo and S. Nagamori, “Permanent-Magnet and Brushless DC Motors”, Clarendon Press Oxford 1985.

[6] SEM Controlled Motor Technology, Series HD, Brushless DC/AC Servomotors, SEM/G/94/50.

[7] Kollmorgen Seidel GmbH & Co. KG, GOLDlINE BH Series, Brushless DC Motors, (www.kollmorgen-seidel.de).

[8] Gordon R. Slemon, ”Electrical Machines for Variable-Frequency Drives”, IEEE Proceedings, Vol. 82, No. 8. August 1994.

[9] ABB, Servomotors and Drives, BIVECTOR 500, Series 8C, PM synchronous motors, YOO 1/2000.

[10] Kollmorgen Seidel GmbH & Co. KG, GOLDlINE SM Series, PM synchronous motors, (www.kollmorgen-seidel.de).

[11] Antonio Fratta and Alfredo Vagati, “A Reluctance Motor Drive for High Dynamic Perfromance Applications”, IEEE Transactions on Industry Applications, Vol. 28, No. 4, July/August 1992.

[12] Antonio Fratta, Cornel Petrache, Giovanni Franceschini and GianPiero Troglia, “A Simple Current Regulator for Flux-Weakened operation of high performance Synchronous Reluctance Drives”, IEEE 1994.

[13] Guru & Hiziroglu, “Electric Machinery and Transformers”, Oxford University Press 1995.

[14] Pekka Tiitinen, “The next generation Motor Control method, DTC Direct Torque Control”, Power Electronics, Drives and Energy Systems for industrial Growth, 1996, Volume: 1 , 1995.

[15] ABB, IEC Low-voltage Induction Motors, Series M2AA, ABB Automation /Cat. BU/400V 50 Hz GB 00-03.

[16] Lenze, Global Drive asynchronous servo motors, Series MDSKA/MDFKA, (www.lenze.de).

[17] SEM Controlled Motor Technology, Series MT, PM DC Servomotors, SEM/A/93/37.

[18] Rajan Mathew, Dan Houghton, and Wardina Oghanna, "Vector Control Techniques for Induction Motors", IEEE Catalogue No. 95TH8025, 1995.

[19] Pyrhönen Juha, "Moottorit sähkökäytöissä", LTKK, sähkötekniikanlaitos, Lappeenranta 1995.

[20] Slemon Gordon R. "Electric machines and drives", ISBN: 0-201-57885-9 Addison-Wesley, cop. 1992

[21] Gunnar Bolmsjö, Håkan Neveryd, and Håkan Eftring "Robotics in rehabilitation", IEEE transactions on rehabilitation engineering, Vol. 3, No. 1, march 1995.

[22] Paolo Dario, Eugenio Guglielmelli, and Benedetto Allotta "Robotics in medicine", ARTS Lab, Italy.

[23] John L. Dallaway, Robin D. Jackson, and Paul H. A. Timmers "Rehabilitation robotics in Europe", IEEE transactions on rehabilitation engineering, Vol. 3, No. 1, march 1995.

[24] ABB Industry Oy, ACS 600 SingleDrive Frequency Converters Technical Catalogue, 2000-06-09 EN.

[25] TRASMITAL BONFIGLIOLI, planetary gearbox series 300, UNI EN ISO 9001-007.

[26] Stegmann, Single –Turn Absolute Encoder (www.stegmann.com).

[27] Richard M. Crowder "Electric Drives and their Controls", Clarendon Press Oxford 1995.

[28] Mård Matti "Sähkökäyttö ja Tehoelektroniikka", Otatieto 889, ISBN 951-672-156-7, Gummerus Kirjapaino Oy, Jyväskylä, 1993.

APPENDIX A

Drive Simulation Model

Figure (A.1) shows the drive simulation model which is based on Figure (3.3). The motor torque is assumed to have a fast torque response and therefore it is represented here by a step function with a worst case rise time of 10 ms. The load torque shown steps in zero seconds to its maximum value given in Table (3.1). The resultant speed is multiplied by a factor of 57.3 to convert it from radians/seconds to degrees/seconds and divided by the gear ratio to find out the speed on the drive load side.

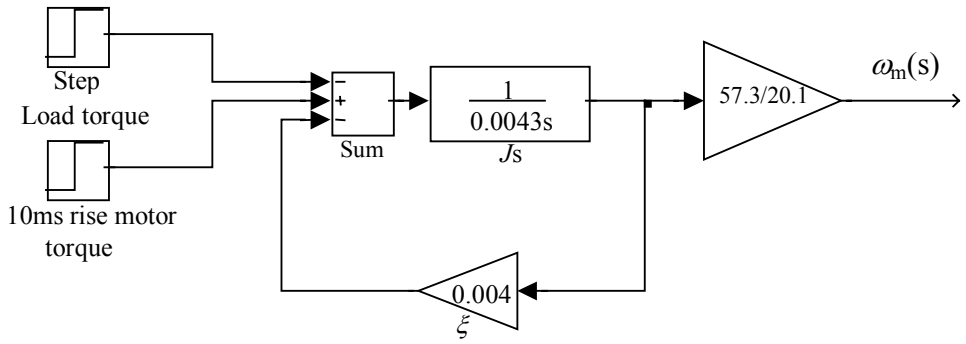

Figure A.1. The simulation model of the prototype drive. The output speed is the speed on the drive load side.

The value of the damping constant (ξ) was calculated based on Equation (3.1). The drive (motor, gear, and load mechanism) was run at no load and constant speed of 1200 rpm (125.66 rad/s). Under this condition the driving torque recorded was 0.5 Nm. When the drive is run with no load and constant speed, Equation (3.1) reduces to:

$$T_{\mathrm{m}} = \xi\, \omega_{\boldsymbol{m}} \tag{A.1}$$

From Equation (A.1), the value of the damping constant is

$$\xi = \frac{T_{\mathrm{m}}}{\omega_{\mathrm{m}}} = \frac{0.5}{125.66} \cong 0.004 \mathrm{Nm\,rad^{-1}s}$$

APPENDIX B

Key Parameters

Below is a list of the drive key parameters with their optimized values that corresponds to the prototype drive. The list is restricted to those parameters which were changed (optimized) during the drive commissioning and testing.

The frequency converter manufacturer (ABB) provides a list of all the parameters available with their corresponding default values.

Parameter	Description	Value
99.01 LANGUAGE		ENGLISH
99.02 APPLICATION MACRO	The application macro used.	Position
99.04 I/O CONFIGURATION	The hardware configuration used.	NIOCP_SSI2
99.05 MOTOR NOM VOLTAGE	Motor nominal voltage.	400 V
99.06 MOTOR NOM CURRENT	Motor nominal current (I_{2hd} =11 A).	3.45 A
99.07 MOTOR NOM FREQ	Motor nominal frequency.	50 Hz
99.08 MOTOR NOM SPEED	Motor nominal speed.	1420 rpm
99.09 MOTOR NOM POWER	Motor nominal power.	1.5 kW
10.04 STOP FUNCTION	Defines the way the motor is stopped.	RAMP
10.05 C_RAPID STOP NOT	Emergency RAPID stop function.	DI2
11.03 TORQUE LIM1 SEL	Selects the torque limit source.	MX TORQUE 1
20.01 MIN SPEED REF	Minimum driving speed.	-1420 rpm
20.02 MAX SPEED REF	Maximum driving speed. 270 , 360°/s.	1420 rpm
20.03 MAX CURRENT	The current the ACP600 will supply to the motor.	150%
20.04 MAX TORQUE 1	Maximum torque limit.	80% - 100%
20.06 C_TRQUE LIM SWITCH	Defines the source of the online torque limit switch.	OFF
20.07 OVERVOLTAGE CTRL	We use a braking resistor so it should be disabled.	OFF
20.08 UNDERVOLTAGE CTRL		ON
20.09 C_POSIT SPD ENABLE	Source for the positive speed reference enable.	DI6
20.10 C_NEGAT SPD ENABLE	Same as 20.09	DI7
20.11 MIN POSITION	Minimum position limit.	0
20.12 MAX POSITION	Maximum position limit.	180
20.13 POS POSIT SPEED	Maximum positive positioning speed.	70

Continue …		
20.14 POS NEGAT SPEED	Maximum negative positioning speed.	-70
20.15 POS ACCELER LIM	Maximum positioning acceleration	
20.16 POS DECELER LIM	Maximum positioning deceleration.	
22.02 ACCELER TIME 1	Acceleration time.	0.1 s
22.03 DECELER TIME 1	Deceleration time.	0.1 s
23.03 INTEGRATION TIME 1	The integration time for the speed PI controller.	146.6 ms
23.11 ACT SPEED SEL	The source of the actual speed.	ESTEMATED
28.01 C_POS ENABLE SEL	Position interpolator is always enabled.	YES
28.02 C_POSIT START SEL	Define the source of the positioning start command.	TRUE/SPECIAL
28.03 POSITION FORMAT	Selects the type of the positioning application.	ROLLOVER AXIS
28.04 POS SCALE METHOD	It defines the scaling method used.	DEGREE
28.06 POS REF FILTER T	Reduce jerk caused by positioning process.	0 ms
28.07 POS CONTROL GAIN	The gain of the position control loop.	949.5 min^{-1}
28.07 SPEED FEED FOROW	The speed feed forward behavior.	30 %
28.10 POSITIONING SPEED	It sets the positioning speed.	
28.11 POS ACCELERATION	Maximum positioning acceleration.	
28.12 POS DECELERATION	Maximum positioning deceleration.	
50.03 MOTOR GEAR COUNT	Motor gear numerator.	201
50.04 MOTOR GEAR DENOM	Motor gear denominator.	10
50.10 SSI SHFT POS BITS	Position within one revolution (power of 2).	14
50.11 SSI TOTAL BITS	Length of the whole SSI message.	14

APPENDIX C

Auxiliary Equipment

Some of the auxiliary equipment used in the prototype drive were not mentioned within the text. Below is a list of these equipment and their corresponding technical data.

Braking chopper	
Type:	NBRA-653
Manufacturer:	ABB
Dimensions:	Height: 198.5 mm, Width: 157 mm, Depth: 149 mm.
Weight:	2.9 kg
Braking resistor	
Type:	SACE08RE44
Manufacturer:	ABB
Dimensions:	Height: 365 mm, Width: 290 mm, Depth: 131 mm.
Weight:	6.1 kg
Absolute encoder adapter	
Type:	NSSIP-01
Manufacturer:	ABB Industry Oy
Lever arm	
Manufacturer:	Diter
Load cell	
Type:	Z6FD1/500kg
Provider:	Oy Transmotic Ab
Amplifier	
Type:	WE2110, 2*RS-232
Provider:	Oy Transmotic Ab
Inductive switches	
Type:	SKS-product number: 9982-4600 PNP
Manufacturer:	SKS

APPENDIX D

Drive Wiring Layout

Figure (D.1) shows detailed electrical connections of the different components making up the prototype drive. The connection shown for the inductive switch is given only for demonstration purposes, in fact, there are three more inductive switches available in this design, and they can be connected in the same manner.

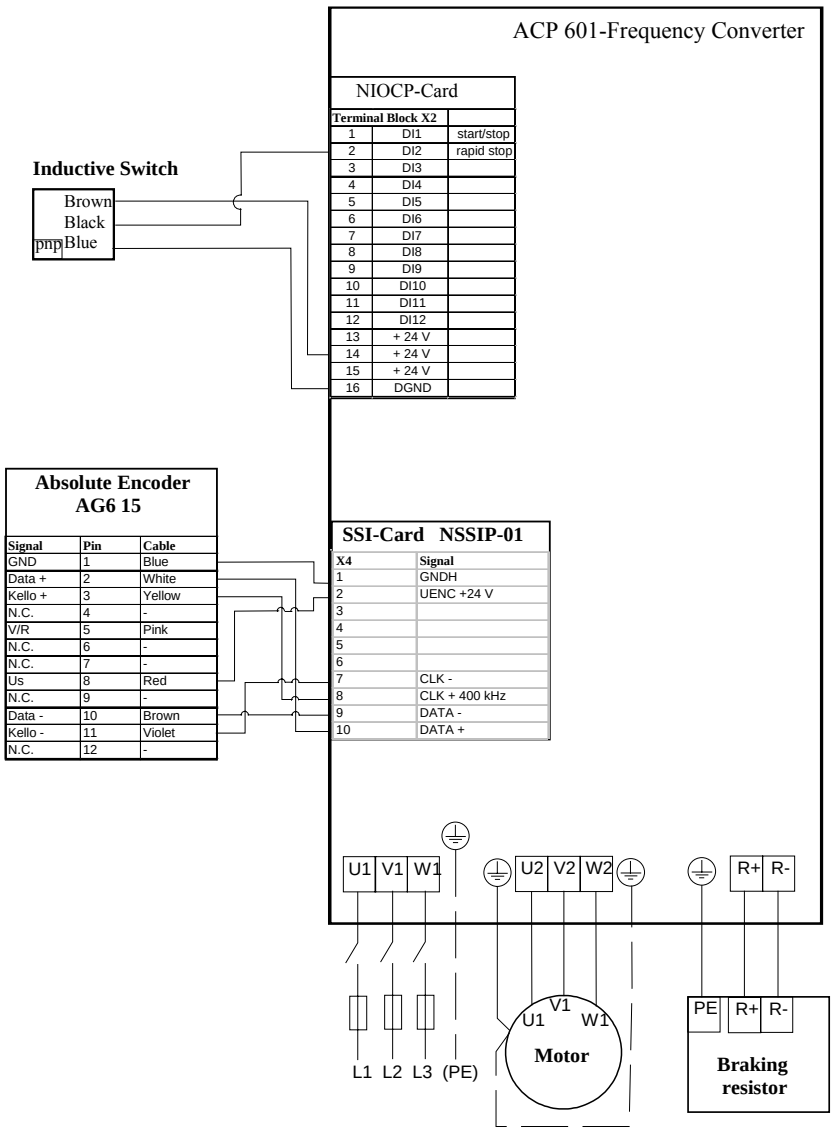

Figure (D.1). The electrical wiring layout of the prototype drive.

APPENDIX E

Snapshots of the Prototype Drive

Figure (E.1) is a snapshot of the real test bench used to carry out the prototype drive test. The drive load shaft is connected to the shaft of a large dc machine (item 1) through a long shaft connector (item 2), the actual speed and torque at the shaft are monitored throughout the testing process.

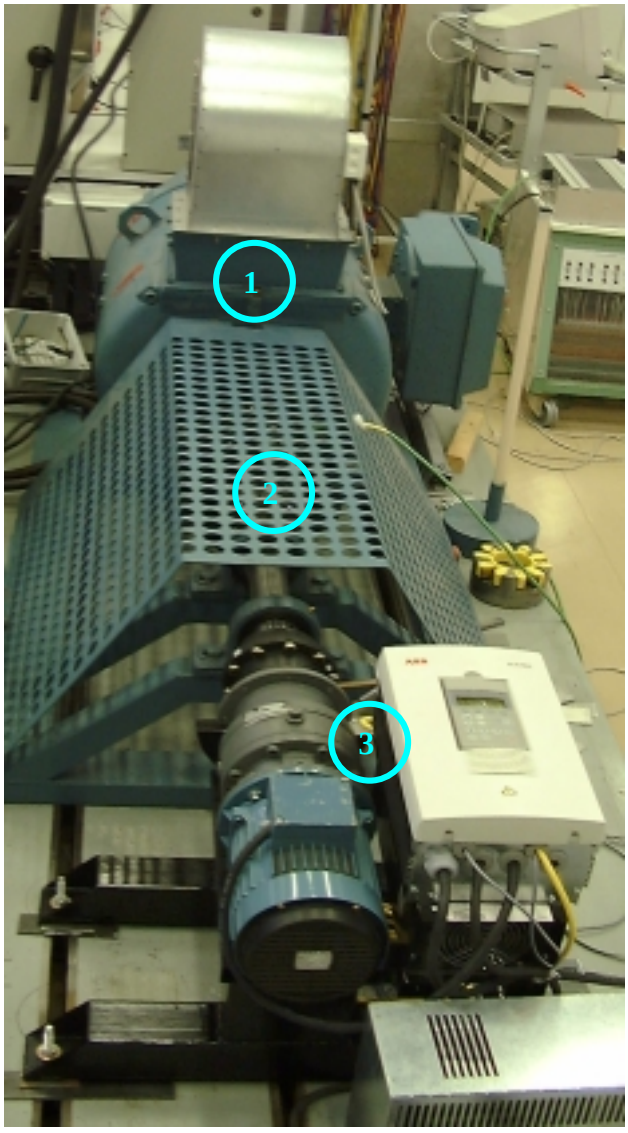

Figure (E.1). The real test bench, the numbers are: 1- The dc machine (Load machine). 2- The shaft connector. 3- The prototype drive.

Figure (E.2) is another snapshot of the prototype drive, but this time with its real load mechanism and a close look at the different components and their assembly.

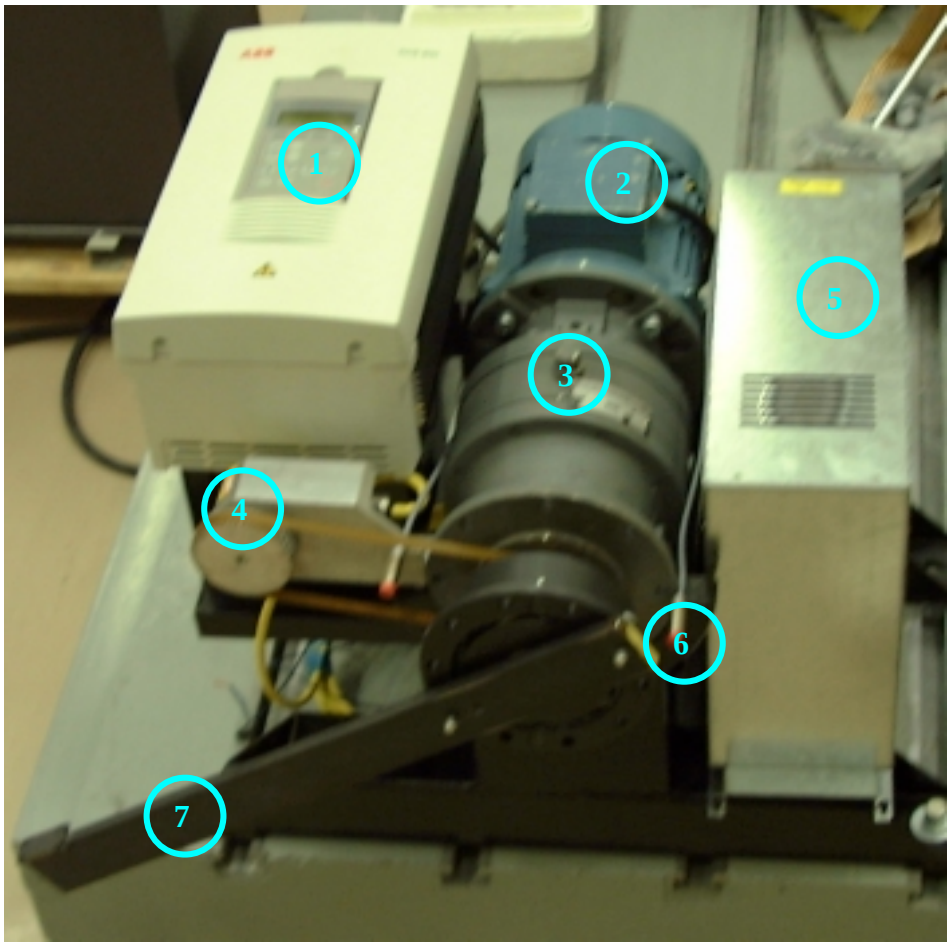

Figure E.2 Assembly of the Prototype drive. The components are numbered as: 1- Frequency converter (ACP 600). 2- Squirrel-cage induction motor. 3- Planetary gearbox. 4- The position absolute encoder and its belt-drive connection to the load shaft. 5- Braking resistor. 6- Inductive safety switch. 7- Lever arm.